Published in final edited form as:
Dev Biol. 2009 June 1; 330(1): 54–72. doi:10.1016/j.ydbio.2009.03.009.

Restricted patterns of Hoxd10 and Hoxd11 set segmental differences in motoneuron subtype complement in the lumbosacral spinal cord

Mala Misra[1], **Veeral Shah**[1], **Ellen Carpenter**[2], **Peter McCaffery**[3], and **Cynthia Lance-Jones**[1]

1*Department of Neurobiology and Center for Neuroscience, University of Pittsburgh School of Medicine, Pittsburgh, Pennsylvania 15261*

2*Mental Retardation Research Center, Department of Psychiatry and Biobehavioral Science, UCLA School of Medicine, NRB 303, 635 Charles E. Young Drive South, Los Angeles, CA 90095*

3*Institute of Medical Science, University of Aberdeen, Foresterhill, Aberdeen, AB25 2ZD, UK*

Abstract

During normal vertebrate development, Hoxd10 and Hoxd11 are expressed by differentiating motoneurons in restricted patterns along the rostrocaudal axis of the lumbosacral (LS) spinal cord. To assess the roles of these genes in the attainment of motoneuron subtypes characteristic of LS subdomains, we examined subtype complement after overexpression of Hoxd10 or Hoxd11 in the embryonic chick LS cord and in a Hoxd10 loss-of-function mouse embryo. Data presented here provide evidence that Hoxd10 defines the position of the lateral motor column (LMC) as a whole and, in rostral LS segments, specifically promotes the development of motoneurons of the lateral subdivision of the lateral motor column (LMCl). In contrast, Hoxd11 appears to impart a caudal and medial LMC (LMCm) identity to some motoneurons and molecular profiles suggestive of a suppression of LMC development in others. We also provide evidence that Hoxd11 suppresses the expression of Hoxd10 and the retinoic acid synthetic enzyme, retinaldehyde dehydrogenase 2 (RALDH2). In a normal chick embryo, Hoxd10 and RALDH2 are expressed throughout the LS region at early stages of motoneuron differentiation but their levels decline in Hoxd11-expressing caudal LS segments that ultimately contain few LMCl motoneurons. We hypothesize that one of the roles played by Hoxd11 is to modulate Hoxd10 and local retinoic acid levels and thus, perhaps define the caudal boundaries of the LMC and its subtype complement.

Keywords

neural tube development; LIM genes; RALDH2; lateral motor column; pattern formation; fate determination

Direct correspondence to: Cynthia Lance-Jones, Department of Neurobiology, University of Pittsburgh School of Medicine, Biomedical Science Tower 1, W1442, 3500 Terrace Street, Pittsburgh, PA 15261, Telephone: 412 648-9078, Fax: 412 648-1441, E-mail: E-mail: clancej@pitt.edu.

INTRODUCTION

A critical first step in the formation of neural circuits is the establishment of molecular differences between groups of developing neurons that then lead to unique patterns of cellular organization and synaptic connectivity. The motoneurons of the vertebrate spinal cord provide an excellent model for defining mechanisms of cell type diversification because of clear associations between cell body position, target identity and molecular profile (see Eisen, 1999; Jessell, 2000; Landmesser, 2001; Shirasaki and Pfaff, 2002; di Sanguinetto et al., 2008). In birds and mammals, motoneurons projecting to different target fields are located in discrete columns and each axial level of the spinal cord contains a unique complement of these columns. Visceral sympathetics form an intermediately positioned column restricted to thoracic segments. Somatic limb-innervating motoneurons form the lateral motor column (LMC) within brachial and lumbosacral (LS) segments, while somatic non-limb innervating motoneurons of the medial motor column (MMC) are broadly distributed along the rostrocaudal axis. Somatic motor columns are split secondarily into lateral and medial divisions; the LMC consists of divisions projecting to dorsal and ventral limb musculature (the LMCl and LMCm), the MMC of divisions projecting to body wall and axial musculature (the MMCl and MMCm, respectively). Finally, each division consists of pools of motoneurons that project to individual muscles.

A combinatorial code of LIM homeodomain proteins distinguishes spinal motor columns and their divisions (Tsuchida et al., 1994; Jessell, 2000). Stereotyped patterns of LIM expression as well as motor projections are programmed at early neural tube stages (Matise et al., 1996; Ensini et al., 1998; Lance-Jones et al., 2001). Functional analyses indicate that LIM proteins play roles in the triggering of motoneuron differentiation (Lee and Pfaff, 2003; Hutchinson and Eisen, 2006), the specification of subtype identity (Kania et al., 2000, Sharma et al., 2000; Thaler et al., 2004), and the regulation of guidance molecules critical for axon pathway choice (Kania and Jessell, 2003; Shirasaki et al., 2006). In conjunction with LIM proteins, the expression of other transcription factors, including the ETS proteins, Er81 and Pea3 (Lin et al., 1998; Livet et al., 2002), the runt-related protein, Runx1, the Pou-domain factor, Scip (Dasen et al., 2005) and the homeodomain protein, Nkx6.1 (DeMarco Garcia and Jessell, 2008), distinguishes motoneuron subtypes at the level of individual motor pools.

With the recognition of the early diversity and functional importance of specific transcription factors comes the question of how their expression patterns are established. Members of the Hox family of homeodomain proteins have been shown to direct the diversification of motoneuron subtypes in individual hindbrain segments, influencing both transcription factor profile and axon trajectory (Lumsden and Krumlauf, 1996; Cooper et al., 2003; Briscoe and Wilkinson, 2004; Guthrie, 2007). Studies by Ensini et al. (1998), Liu et al. (2001), and Dasen et al. (2003, 2005, 2008) provide evidence that a network of Hox proteins are involved in motoneuron diversification at brachial and thoracic spinal levels in the chick embryo. For example, the restricted expression of Hox6 and Hox9 proteins sets patterns of LIM expression distinguishing brachial motor columns as a unit, while Hox3, 4, 5, 7, and 8 proteins set pool-specific transcription factor and axon projection patterns characteristic of rostral and caudal subdomains within the brachial region. Data from mammalian models further implicate Hox genes in brachial motoneuron development, as mice lacking Hoxc8 function show specific losses in LIM- and ETS-defined motoneuron subtypes and defects in peripheral nerve projections at brachial spinal levels (Tiret et al., 1998; Vermot et al., 2005).

At caudal spinal levels, Hox10 paralogues are expressed throughout hindlimb-innervating segments and are clearly involved in defining the rostral position of the lumbar region. Mice lacking Hoxa10 and/or Hoxd10 function and Hoxc10/Hoxd10 knockout mice show shifts in the position of the thoraco-lumbar border as well as alterations in peripheral nerve morphology

(Rijli et al., 1995; Carpenter et al., 1997; de la Cruz et al., 1999; Wahba et al., 2001; Lin and Carpenter, 2003; Tarchini et al., 2005; Wu et al., 2008). Further, ectopic expression of Hoxd10 in chick thoracic neural segments induces motoneurons with a lumbosacral-like molecular profile and novel axonal projections to hindlimb muscles (Shah et al., 2004). Recent analyses of motoneuron development in double knockout mice (Wu et al., 2008) implicate Hoxc10 and Hoxd10 in the establishment of Lim1+ LMCl motoneurons, but little is known about the individual roles of caudal Hox proteins in subtype specification. We have examined motoneuron subtype complement after Hoxd10 or Hoxd11 overexpression in the chick LS spinal cord and in a Hoxd10 loss-of-function mouse (Carpenter et al. 1997). Our findings suggest that Hoxd10 expression is critical to the definition of LMC boundaries and that it ultimately promotes the development of LMCl motoneurons, a characteristic feature of rostral LS or lumbar segments. We also present data suggesting a two-fold role for Hoxd11. This gene is uniquely expressed in caudal LS segments and appears to promote the development of at least one caudal motor pool. However, our data also suggests that Hoxd11 represses Hoxd10 and RALDH2 expression and in so doing indirectly influences the positioning and differentiation of LMC and MMC motoneurons within caudal spinal segments. Aspects of this work have been published in abstract form (Misra et al., 2005; Misra and Lance-Jones, 2008).

MATERIALS AND METHODS

Experimental Animals

Chick embryos—Fertilized chick eggs (CBT Farms, Chestertown, MD) were incubated in a forced-draft incubator at 98°F. Eggs to be used for *in* ovo electroporation were opened at embryonic days (E) 2.5, and a 0.5% neutral red in physiological saline applied to the embryo to increase visibility and facilitate stage assessment. Following electroporation, eggs were incubated until E4-7 (stages 22-30 of Hamburger and Hamilton, 1951). At sacrifice, embryos were placed in cold avian saline, staged, and dissected to a trunk/limb preparation. E4-7 embryos were used for assessment of normal molecular profiles.

Mouse embryos—The generation of Hoxd10 mutant mice has been described previously (Carpenter et al., 1997). E12.5-E13.5 embryos were collected from timed pregnancies resulting from heterozygous intercrosses. For genotyping, DNA isolated from tail biopsies was analyzed using PCR-amplified DNA as described (Wahba et al, 2001). Photos of retrogradely labeled motoneurons from E12.5-E13.5 CD1 mouse embryos are included to illustrate selected motor pool positions. This tissue was prepared for prior studies of motor column development in the mouse lumbar cord (Lance-Jones, 1982; Lance-Jones, 1984).

In ovo electroporation

Neural tubes from stage 14-16 chick embryos were microinjected at future LS levels with 1.25 μg/ul DNA constructs encoding Hoxd10+EGFP, Hoxd11+EGFP, or EGFP alone. DNA was diluted with Tris-EDTA, pH 8.0, with 0.05% Fast green for visibility during injection. Following injection, embryos were bathed in sterile saline and electroporated using gold 0.5 mm electrodes. Electrodes were positioned on either side of the neural tube such that one half of the neural tube was transfected. Current was delivered in 3 pulses (50 millisecond duration, charging voltage of 17V) by a square pulse electroporator (BTX).

DNA constructs

One set of constructs was made by cloning full-length chicken *hoxd10* or *hoxd11* (provided by C. Tabin) into the pMES vector (provided by C. Krull). The pMES vector consists of pCAX (Kobayashi) with the addition of the *ires-egfp* fragment from pIRES2-EGFP (Clontech). Gene expression is driven ubiquitously at high levels in progenitor and postmitotic neural cells by a

β-actin promoter. A second group of constructs was generated by inserting full-length *hoxd10* or *hoxd11* and the *ires-egfp* fragment from pIRES2-EGFP, in frame, into a pBluescript-based vector containing the 9kb Hb9 promoter (provided by S. Pfaff), which drives gene expression specifically in postmitotic motoneurons (Arber et al., 1999, Thaler et al., 1999). *Hoxd10* and *hoxd11* were also cloned into an alternate Hb9 vector containing an abbreviated Hb9 promoter sequence and a minimal CMV enhancer (also provided by S. Pfaff). Results derived from experiments in which Hox overexpression was driven by the full-length Hb9 promoter did not differ from those of equivalent experiments with the abbreviated Hb9 promoter. Data from the two types of Hb9 constructs were therefore pooled.

Immunohistochemistry and in situ hybridization

Tissues from both chick and mouse embryos were fixed in 4% paraformaldehyde for 1.5-2 hours, cryoprotected in 30% sucrose, embedded in 50:50 30% sucrose:OCT, frozen, and sectioned at 14 μm. Serial transverse sections were placed on three sets of slides in an alternating pattern to permit processing of adjacent sections with different antibodies or mRNA probe combinations. The following antibodies were used at the indicated dilutions: rabbit anti-Hb9, 1:8000, rabbit anti-Lim3, 1:2500 (S. Pfaff); guinea pig anti-Hoxd10, 1:8000, rabbit anti-Hoxd11, 1:16000, rabbit anti-Lim1, 1:40000, guinea pig anti-Scip, 1:8000, rabbit anti-Foxp1, 1:32000, rabbit anti-Pea3, 1:8000, rabbit anti-Chx10, 1:4000 (T. Jessell); rabbit anti-EGFP, 1:1500, mouse anti-EGFP, 1:500 (Invitrogen); goat anti-EGFP, 1:500 (Rockland Immunochemicals); mouse anti-Isl1(2), 1:100, mouse anti-Lim3, 1:100, mouse anti-neurofilament, 1:100 (DSHB); anti-nNOS, 1:5000 (Immunostar); and rabbit anti-RALDH2, 1:2500 (P. McCaffery). Cy2-, Cy3-, and Cy5-conjugated secondary antibodies (Jackson Immunoresearch) were used for fluorescent imaging. For bright field imaging, 3,3-diaminobenzidine (DAB) immunoprocessing with an ABC kit (Vector Laboratories) was used. In situ hybridization was used to characterize Hox (C. Tabin), Isl1 (T. Jessell), and Slit2 (J. Raper) expression in chick cord sections or whole mounts. Digoxygenin-labeled RNA probes were synthesized according to the supplier's protocol (Roche Applied Sciences) and hybridization performed using modified protocols of Nieto et al. (1996) and Schaeren-Wiemers and Gerfin-Moser (1993).

Retrograde labeling

We employed standard retrograde labeling techniques (Landmesser, 1978) with 10% rhodamine-conjugated dextran in 0.5% Triton-X/saline solution. (Yip et al., 1998) to identify motor pool patterns in stage 29-30 chick embryos. Procedures for the retrograde labeling of motoneurons in E13.5 mouse embryos were similar to those for the chick with some exceptions. Muscle complexes were injected with 20% HRP (Sigma Type VI) in a 1% lysolecithin/saline solution and the tissue incubated in mammalian physiological saline at room temperature. After fixation in 2% glutaraldehyde, tissues were embedded in gelatin/albumin and then 30% sucrose, frozen, and sectioned at 40μm with a sledge microtome. Mounted sections were processed using standard cobalt intensified-DAB procedures and counterstained with 0.5% cresyl violet.

Cell Quantification

Chick—Counts of cells expressing LIM proteins or transcripts and/or EGFP were made on transverse sections through identified LS segments in stage 23-25 and/or stage 29 embryos. Segment number and boundaries were identified by reference to dorsal root ganglia and spinal nerves on the non-transfected side. Three sections per segment were chosen for counting based on their position in that segment (i.e. three sections equidistant from one another in the middle of a segment). Somatic motoneuron status was assigned to Isl1(2)+ cells located within three nuclear-widths of the dorsal edge of the visible somatic motor column cluster. Motoneuron

subtype identity was established through assessment of staining with anti-Lim1, Lim3, Isl1(2). Foxp1, Pea3 and Scip antibodies and an *Isl1* RNA probe. In triple-labeled sections, Isl1(2) staining was in some cases divided into Isl1(2)^{high} and Isl1(2)^{low}. Isl1(2)^{high}+ motoneurons were distinguished in micrographs by pixel intensity above a fixed threshold. The value of this threshold was equivalent to the value at which all Lim1+, Isl1(2)^{low} were excluded from the group (see Fig. 3). To quantify the spatial positions of transfected motoneurons, a grid was superimposed on the ventral spinal cord (see Fig. 3). The medial edge and dorsal edges of the grid were aligned with the ventricular zone and the dorsal edge of the LMC cluster, respectively. The lateral edge of the grid was aligned with the lateral edge of the LMC cluster such that the dorsoventral midpoint of the grid coincided with the widest point in the spinal cord. Motor regions chosen for assessments were those where RALDH2 is normally high and where the density of Isl1(2)+ cells appeared equivalent under control and experimental conditions. To assess RALDH2 expression, sections were stained with anti-RALDH2 and anti-Isl1(2) and mean pixel intensity of anti-RALDH2 fluorescence measured (NIH ImageJ, 1.37v) in circumscribed motor regions. To assess the rostrocaudal distribution of dextran+ motoneurons following retrograde labeling, counts were made on non-adjacent 14 μm horizontal sections of stage 29-30 Hb9::d11 embryos. Anti-Chx10 staining was used for the identification and counting of V2a interneurons.

Mouse—Counts of LMC and MMC motoneuron subtypes were made on transverse 14 μm cord sections stained with anti-Hb9 and Isl1(2) or anti-nNOS and Isl1(2). Individual segments were identified by reference to the ribs, prior investigations having shown that rib patterns were unchanged in the homozygous Hoxd10 mutants (Carpenter et al., 1997). For each embryo, photos were taken of one half of the ventral cord at the mid level of spinal nerve exit for T12-L6. Counts of LMC motoneurons were limited to profiles located within the morphological somatic motor column cluster or within 3 nuclear diameters of its edge.

Microscopy and photography

Most fluorescence and bright-field microscopy was carried out using a Nikon Eclipse E600 compound microscope and a QImaging Retiga 2000R camera. Tissue sections labeled with three antibodies were examined and photographed using an Olympus Fluoview FV1000 confocal unit fitted to an Olympus BX61 microscope. Cells showing specific molecular profiles were dotted in Photoshop and labeled images imported into a counting program (designed by Nicholas Roy, Massachusetts Institute of Technology, Cambridge, MA).

RESULTS

Segmental patterns of Hoxd10 and Hoxd11 expression in the chick embryo

The distribution of *Hoxd10* transcripts in the developing chick spinal cord has been described (Lance-Jones et al., 2001), but limited information (Dasen et al., 2005) is available for Hoxd10 protein expression or for Hoxd11. We therefore began with an assessment of normal Hoxd10 and Hoxd11 patterns at two embryonic stages. Stage 24 represents an early stage in the process of LS motor column formation. Molecular differences between motoneuron subtypes have begun to appear but LMCl motoneurons have yet to migrate past LMCm motoneurons (Fig. 1A-C). At stage 24, Hoxd10 is expressed in all LS segments, while Hoxd11 is expressed only in caudal segments (Fig. 1D-I). Within their respective rostrocaudal domains, the expression of each gene is widespread within motoneuron populations, being absent only in the most recently born (most medial) cells (Fig. 1J-K). In caudal segments, most but not all motoneurons appear to express both Hoxd10 and Hoxd11 (Fig. 1L). Stage 29 represents a stage when LS motoneurons have settled in adult-like positions in the ventral horn (Fig. 1M-O), but the major period of cell death has yet to occur (Hamburger and Oppenheim, 1982). At stage 29, the expression of Hoxd10 is evident in subsets of motoneurons in LS1-5, but few if any motor

neurons express Hoxd10 at LS6+ levels (Fig. 1P-R). In contrast, motoneuron expression of Hoxd11 begins in LS4/5 and is widespread at L6+ levels (Fig. 1S-U).

Hoxd10 overexpression in the chick LS neural tube shifts the segmental complement of motoneuron subtypes toward LMCl

Prior studies suggest that Hoxd10 plays an instructive role in defining broad LMC character and position (Carpenter et al., 1997; Shah et al., 2004). However, recent analyses of mutants with the loss of both Hoxc10 and Hoxd10 function (Wu et al., 2008) raise the possibility that Hoxd10 also specifically promotes LMCl development. In a normal embryo, most LMCl motoneurons can be defined by their expression of Lim1 and their projections to dorsal limb musculature (Tsuchida et al., 1994). We noted that rostral LS segments, which express high levels of Hoxd10, contain a larger complement of Lim1+ motoneurons than caudal segments at stage 29. This difference is likely to persist because rostral segments contain substantially more dorsally projecting motoneurons than caudal segments at stage 36 (Fig. 1V). These observations raise the possibility that Hoxd10 is instrumental in defining this distinguishing feature of rostral LS segments.

To test this hypothesis, we asked if overexpression in chick LS segments would influence LS motoneuron subtype complement in a manner predicted by normal expression. Full-length *hoxd10*, along with the *ires-egfp* sequence from pIRES2-EGFP (Clontech), was cloned into vectors that drive gene expression under the postmitotic motoneuron-specific Hb9 promoter (Arber et al., 1999; Thaler et al., 1999). A construct expressing EGFP alone under the same promoter was used as a control. Constructs were transfected into the neural tube via in ovo electroporation before motoneurons are born (stages 14-16, Hollyday and Hamburger, 1977) and most embryos were sacrified either at early stages of motoneuron differentiation (stages 22-early 25) or after motor column formation (stages 29-30). While evidence of transfection was often present in multiple LS segments, we focused mainly on LS2 for assessments of motoneuron subtype complement.

Endogenous Hb9 is expressed by all motoneurons immediately following their exit from the ventricular zone (Tanabe et al., 1998; Thaler et al., 1999, Arber et al., 1999). It is widely expressed at stages 22-24 but by stage 29, maintained only in a subset of motoneurons (William et al., 2003). At stages 24, evidence of Hoxd10 overexpression and colocalization with EGFP was readily detected, although a decreasing medial to lateral gradient of Hoxd10 expression suggests that the earliest born (more lateral) motoneurons may have begun to lose Hoxd10 expression (Fig. 2A-B). To assess the effect of this early increase in Hoxd10, LS2 sections from stage 23-early 25 Hb9::d10 embryos were immunolabeled with antibodies against Isl1 (2), a panmotoneuron marker, and Lim1, a marker for LMCl motoneurons (Tsuchida et al., 2004), as well as EGFP (Fig. 2C). In this and all subsequent experiments, counts of motoneurons were made on three non-adjacent sections per embryo with 4-6 embryos making up each experimental group (Table 1). In stage 23-early 25 Hb9::d10 embryos, we found no difference in the mean total number of motoneurons per section between transfected and non-transfected sides (Fig. 2D). However, a significant increase in the mean number of Lim1+ motoneurons was present (Fig. 2E-F). Further, while Lim1+ motoneurons made up only 29% of the total motoneuron population on the transfected side, they made up 42% of the transfected (EGFP+) population (Table 1). These data are compatible with the hypothesis that Hoxd10 overexpression initiated an early fate switch from medial (LMCm or MMC) to lateral (LMCl) motoneuron differentiation pathways. To discriminate between an LMCm-to-LMCl vs. an MMC-to-LMCl switch, transfected LS2 sections were immunolabeled with Foxp1, a Forkhead domain transcription factor that is normally expressed by both LMCl and LMCm motoneurons, but not by MMC motoneurons (Rousso et al., 2008; Dasen et al., 2008). Total numbers of

Foxp1+, Isl1(2)+ cells were similar on transfected and non-transfected sides, suggesting an LMCm-to-LMCl switch (Figs. 2G-I, Table 1).

Transfected LS2 sections were also examined in stage 29 Hb9::d10 embryos. Unlike in stage 23-25 embryos, visible signs of Hoxd10 overexpression were absent (Fig. 2J-K) and counts of both total motoneuron numbers and Lim1+ populations were similar on transfected and non-transfected sides (Fig. 2M-R, Table 1). These observations suggest that Hoxd10 overexpression under the Hb9 promoter is downregulated at early stages of motoneuron differentiation and that fate changes initiated by Hoxd10 overexpression are transient. The latter implies, in turn, that the early specification of Lim1+ motor neurons is labile. Normally, many LMCl motoneurons in LS2 retain high levels of Hoxd10 through stage 29 (see Fig. 1M,P) and it is possible that these cells require sustained expression of Hoxd10 to maintain a Lim1+ phenotype.

To determine if sustained Hoxd10 overexpression effects long-term changes in subtype complement, Hoxd10 was cloned into the pMES vector. This vector utilizes a β-actin promoter to drive expression in all neural cells and includes an *ires-egfp* to report protein expression (see Eberhart et al., 2002). In LS2 sections from β-actin::d10 embryos, transfected (EGFP+) cells co-express high levels of Hoxd10 through stage 29 (Fig. 3A-B). A construct expressing EGFP alone under the β-actin promoter was used as a control.

LS2 sections from stage 29 β-actin::d10 embryos were initially stained with anti-Lim1 and anti-Isl1(2) to identify and quantify Lim1+ LMCl motoneurons on transfected and non-transfected sides of the cord (Fig. 3C-D). In a normal embryo, LS2 contains a population of LMCl motoneurons that are Lim1-, but can be distinguished from LMCm and MMC motoneurons by their lack of Isl1 expression (Lin et al., 1998). Staining with a digoxigenin-tagged in situ probe against *Isl1* in combination with anti-Isl1(2) was thus used to specifically identify Isl1+ LMCm + MMC populations (Fig. 3E-F). Counts revealed two notable effects of Hoxd10 overexpression with the β-actin::d10 construct (Fig. 3G, Table 1). First, total motoneuron numbers were reduced by 26% on transfected sides of the cord, with no comparable reduction in β-actin::control embryos. Second, this reduction disproportionately affected the *Isl1*+, LMCm+MMC population such that subtype proportions in the motoneuron population as a whole were shifted in the LMCl direction. *Isl1*+ proportions decrease from 51% to 40% on non-transfected vs. transfected sides while Lim1+ proportions increased from 35% to 43% (Fig. 3H, Table 1). Counts of Lim1+ proportions made in LS5 of Hb9::d10 embryos showed a similar effect (see Table 1).

To examine subtype proportions within transfected populations alone, LS2 sections from β-actin::control and β-actin::d10 embryos were triple labeled with anti-Lim1, -Isl1(2), and -EGFP antibodies (Figs. 3I-N). As above, anti-Lim1 staining allowed the identification of most LMCl motoneurons (Fig. 3I-J). To roughly identify and isolate LMCm + MMC motoneurons from the Lim1- LMCl population, we capitalized on the distribution of fluorescence intensity normally seen in the Isl1(2)+ population. “Brightly” stained Isl1(2)+ cells (Isl1(2)^{high}) appear in medial portions of the motor columns and correspond spatially to the position of *Isl1*+ motoneurons (see Figs. 3M-N, compare to Fig. 3E-F). “Lightly” stained populations (Isl1(2) ^{low}) are located laterally, corresponding to the positions of Lim1+ and Lim1- LMCl populations. We utilized a fluorescence intensity threshold function (see Materials and Methods) to isolate and count Isl1(2)^{high} motoneurons, assuming the number of Isl1(2)^{high} cells to be an approximation of LMCm and MMC, the two Isl1+ populations. As can be seen in Fig. 3O, EGFP+ motoneurons in β-actin::d10 embryos showed an increase in the LMCl:LMCm+MMC ratio that paralleled the increase found in the motor columns as a whole (see Table 1).

Many EGFP+ motoneurons in β-actin::d10 embryos showed two additional LMCl features: lateral position and dorsal axonal projections. We quantified the position of EGFP+ motoneurons by superimposing a tripartite grid over individual LS2 sections (Fig. 3P-R). In β-actin::d10 embryos, most transfected motoneurons were located laterally in accord with an LMCl identity, while transfected motoneurons in β-actin::control embryos showed a more widespread distribution. If the segmental complement of motoneurons has shifted towards an increase in LMCl proportions, then one might expect an increase in the proportion of EGFP+ axons that project to dorsal limb regions in β-actin::d10 embryos. To address this possibility, the paths of EGFP+ and neurofilament+ axons were examined in the anterior (crural) plexus region at stage 29 and at an early stage of muscle nerve formation (stage 26-27). In β-actin::control embryos (n=3, stage 27, n=3, stage 29), EGFP+ axons contributed substantially to both femoral and obturator nerve trunks that project to anterior dorsal and ventral limb regions, respectively (Fig. 3S). While the EGFP+ axonal population is likely to have included some sensory axons originated from transfected neural crest, these observations suggest that our protocols generally resulted in the transfection of both dorsally and ventrally projecting neurons. In half (n=3/6) of the stage 26-27 β-actin::d10 embryos examined, a pattern similar to control was found; however, in the remaining stage 26-27 embryos and in all stage 29 embryos (n=6), most EGFP+ axons appeared to diverge at the crural plexus to project along dorsal pathways (Fig. 3T-U).

In sum, these data clearly indicate a shift in motoneuron complement in the LMCl direction following transfection with the β-actin::d10 construct. The interpretation of these changes however, is confounded by the substantial motoneuron cell death observed. One possible explanation is that the early and high levels of Hox produced by transfection with the β-actin::d10 construct had a toxic effect on all motoneurons. This effect, in turn, may have partially masked a promotion of LMCl subtype differentiation, an influence in line with the observed increase in Lim1+ cells in stage 23-25 Hb9::d10 embryos. It is equally possible, however, that high Hox levels were particularly toxic to those motoneurons that withdrew from the cell cycle early and contained the least diluted foreign DNA. Since LMCm motoneurons are normally born before LMCl motoneurons (Hollyday and Hamburger, 1977), LMCm motoneurons may have been preferentially lost due to this toxicity. Given this possibility, we sought to complement our overexpression analyses with an assessment of motoneuron subtype development using a Hoxd10 loss-of-function paradigm.

LMCl motoneuron numbers are reduced in rostral lumbar segments in a Hoxd10 loss of function mouse mutant

In the mouse embryonic spinal cord, Hoxd10 is expressed in lumbar (L) segments (Dolle and Duboule, 1989) and inactivation of Hoxd10 alone or in combination with other Hox10 genes leads to shifts in the position of the thoracic-lumbar boundary (Carpenter et al., 1997; Lin and Carpenter, 2003; Tarchini et al., 2005; Wu et al., 2008). To assess the specific effects of Hoxd10 loss on motoneuron subtypes, we chose to examine subtype distribution in a Hoxd10 loss-of-function mutant in which disruption of the Hoxd10 locus was accomplished via insertion of a neo cassette in exon 2. (Carpenter et al., 1997). Previous descriptions of this mutant indicated alterations in the axial and appendicular skeleton, and peripheral nerve changes, with no apparent changes in either Hoxd9 or Hoxd11 expression (Carpenter et al., 1997). Our central aims were to determine if LMCl motoneuron numbers were reduced with inactivation of Hoxd10 alone, mirroring our Hoxd10 overexpression data, and to determine if such a reduction was restricted to a specific rostrocaudal LS subdomain.

Homozygous mutant embryos and wildtype littermates were collected at E12.5-E13.5, just after lumbar motoneurons are normally born but before the peak period of cell death (Lance-Jones, 1982). To distinguish subtypes, spinal cord sections were double-stained with anti-Hb9

and Isl1(2) (Arber, 1999) or with anti-nNOS and Isl1(2) (Wu et al., 2008). In both mutant and wildtype embryos, the spatial arrangement of subtypes was similar (Fig. 4A-H). Visceral motoneurons were identified as nNOS+, Isl1(2)+ cells in the posterior thoracic (T) and rostral lumbar (L) cord (VM, Fig. 4A). LMCl motoneurons were uniquely identified as Hb9+, Isl1(2)- cells located in the ventral horn cluster. (It should be noted that the Isl1(2) antibody appears to stain only Isl1+ cells in the mouse embryo. See also Wu et al., 2008.) Hb9+, Isl1(2)- cells occupied a lateral position corresponding to the position of motor pools projecting to dorsal limb muscles (Figs. 4E and 4I). LMCm motoneurons were Isl1(2)+, ± low-level expression of Hb9+, and occupied dorsal and medial positions corresponding to the position of many ventrally projecting motor pools (Figs. 4E and 4J). MMC motoneurons showed high expression of both Isl1(2) and Hb9 and occupied a ventromedial position (Fig. 4E). The border between LMCm and MMC motoneurons was identified as a visible space between the two clusters and/or a sharp increase in the level of HB9 staining (see Figs. 4E and 4G).

Counts of individual subtypes were made on one side of the cord in sections taken at the mid level of spinal nerve exit for T12 through L6, sections corresponding roughly to the T12/T13 through LS6/S1 segment borders. The most marked differences between mutant and wildtype littermates were significant decreases in LMCl numbers at rostral levels (T12/13-L2/3; Fig. 4C-D, L). At T12/13-LS1/2, small increases in VM numbers accompanied these LMCl decreases (Fig. 4A-B, K). Although VM increases were not significant, these observations hint at a possible conversion from LMCl to VM. Since a prominent VM is characteristic of thoracic segments, these data suggest a shift from a rostral lumbar to a posterior thoracic identity. In mutants, caudal increases in LMCm motoneuron numbers and decreases in MMC numbers were occasionally found (Fig. 4M-N), an observation also compatible with the idea of a shift in LMC position.

The above observations match prior morphological evidence of a 1/2 segment shift in segment identity in mutant neonates (Carpenter et al., 1997). However, a shift in the position of the LMC as a whole cannot fully account for observed differences between mutant and wildtype numbers. In mutants, there was a significant decline in LMCl numbers when compared to wildtype littermates (+/+ = 281 ± 26 cells, -/- = 245 ± 15 cells, p=0.046). There was, however, no decline in total LMC numbers (+/+ = 645 ± 55 cells, -/- = 639 ± 42 cells), suggesting that an increase in LMCm accompanied the LMCl loss. As they stand, our histograms indicate that changes in LMCl and LMCm numbers occur at different segmental levels (Fig. 4L-M). However, if one assumes a 1/2 segment shift in the position of the mutant LMC and corrects for it by shifting the mutant curves to the left, declines in LMCl numbers at rostral levels (approximately LS2-4) appear to be accompanied by small increases in LMCm numbers, suggestive of conversion from an LMCl to an LMCm identity. In sum, Hoxd10 mutants show evidence of both a shift in the positioning of the T/L boundary and a decrease in the size of the rostral LMCl. The latter observation favors the hypothesis that Hoxd10 biases subtype development towards an LMCl phenotype in rostral LS or lumbar segments.

In the chick embryo, ectopic Hoxd11 expression leads to a reduction in LMCl motoneuron numbers

In the normal chick embryo, Hoxd11 expression is restricted to caudal LS segments. To address Hoxd11 function, we asked if ectopic expression of Hoxd11 in rostral LS segments would lead to the appearance of features normally characteristic of caudal LS segments. Since motor columns within caudal LS segments differ from those of rostral LS segments in that they contain fewer LMCl motoneurons, we asked first if ectopic Hoxd11 expression in rostral LS segments would lead to a decrease in the numbers and/or proportion of LMCl motoneurons. Electroporations were carried out as for Hoxd10 overexpression studies using Hb9- or β-actin-driven constructs. Analyses of subtype complement were made at stage 29 in both Hb9::d11

and β-actin::d11 embryos. Ectopic expression of Hoxd11 was evident in the former (Fig. 5A-D) as well as the latter (data not shown).

In Hb9::d11 embryos, transfected sides of the LS2 cord showed a >40% decrease in Lim1+ (LMCl) motoneurons (Fig. 5G-H, M). This decrease exceeded a small overall decrease in the total Isl1(2) motoneuron population (see Table1; Fig. 5E-F, M). Further, few if any transfected motoneurons were located laterally, in the normal domain of Lim1+ motoneurons (Fig. 5O-Q). Concomitant with a decrease in Lim1+ motoneurons, LS2 sections from Hb9::d11 embryos showed significant increases in the numbers and proportions of Isl1(2)^{high} cells on transfected vs. non-transfected sides (Fig. 5I-J, M-N). This increase was also observed in sections probed for Isl1+ mRNA (Fig. 5K-L).

When transfected (EGFP+) populations were examined in isolation, we found decreases in Lim1+ motoneuron proportions that paralleled those in the motor columns as a whole but were more extreme (Fig. 5N). For example, the ratio of transfected Lim1+ motoneurons in Hb9::d11 embryos vs. Hb9::control embryos was 12%/34%, whereas the equivalent ratio for total Lim1+ motoneurons neurons on transfected vs. non-transfected sides of Hb9:d11 embryos was 25%/37%. Similarly, larger proportionate increases in Isl1(2)^{high} motoneurons were evident in Hb9::d11 embryos when transfected populations were assessed in isolation. These findings suggest that the changes initiated by ectopic Hoxd11 expression arose in part by a cell-autonomous mechanism.

In β-actin::d11 embryo, the decrease in the size of the transfected motor column was substantial, as with β-actin::d10 embryos (Table 1). Nevertheless, in β-actin::d11 embryos, as in Hb9:d11 embryos, the Lim1+ population was disproportionately reduced in both LS2 and LS5. LS2 sections from β-actin::d11 embryos showed significant increases in the proportion of *Isl1*+ motoneurons on transfected vs. non-transfected sides (Table 1). These findings stand in contrast to findings obtained in β-actin::d10 embryos, in which early born, *Isl1*+ motoneurons were disproportionately reduced and late-born Lim1+ motoneurons were preserved. We suggested earlier that the preferential loss of *Isl1*+ motoneurons might be due to a toxic effect on early born cells that underwent few cell cycles after electroporation. The finding of a substantial reduction in late born, Lim1+ motoneurons in β-actin::d11 embryo suggests that any toxic effects of early and high levels of Hox may be unrelated to time of cell cycle withdrawal and that Hoxd10 and Hoxd11 influence progenitors and/or postmitotic cells in quite different ways.

Our data suggest that ectopic Hoxd11 has shifted the subtype complement of rostral LS segments to resemble that of more caudal segments: Lim1+ (LMCl) motoneurons become less prominent, Isl1+ (LMCm+MMC) motoneurons, more prominent. Given that the Isl1+ molecular profile is shared by multiple motoneuron populations, especially early in the differentiation process (Pfaff et al., 1996), we next sought to examine more distinctive markers of caudal segment identity.

Ectopic Hoxd11 expression leads to the appearance of novel axonal projections from rostral LS motoneurons to a caudal thigh muscle

The caudilioflexorius is a thigh muscle normally innervated by LMCm motoneurons located exclusively within the Hoxd11 domain (LS6-8, Landmesser, 1978; Hollyday, 1980). To determine if motoneurons in rostral LS segments would project to the caudilioflexorius after transfection with Hoxd11, we mapped the positions of this motor pool on transfected and non-transfected sides of Hb9::d11 embryos. Muscle injections were performed at stages 29-30 using rhodamine-conjugated dextran as a retrograde tracer. Caudilioflexorius pools on transfected and non-transfected sides were similar in size (n=7, mean pool size on transfected side=210 ± 36 cells, mean pool size on non-transfected side=197 ± 51 cells), and the vast majority of dextran+ motoneurons were located in a normal rostrocaudal position. However, the number

of dextran+ cells located in segments rostral to LS6 was increased on transfected sides (Figs. 6A-B). When expressed as mean percentage of total, dextran+ cells in LS3-5 made up 2±1% of the caudilioflexorius pool on non-transfected sides, but 15.4±6% on transfected sides ($p=0.051$). It is important to point out that EGFP+, dextran+ motoneurons were few in number, most EGFP+ motoneurons being located medial to the caudilioflexorius pool. However, rostrally positioned dextran+ cells on transfected sides appeared to be EGFP+ (Figs. 6C-D). These observations suggest that a small number of transfected motoneurons in rostral segments may have acquired a novel caudal LS identity and been able to reach the caudilioflexorius.

To examine the possibility that Hoxd11 transfection had a global effect on motor pool organization, we mapped the position of motoneurons projecting to the ventral shank complex. In a normal embryo, this group of muscles is innervated by LMCm motoneurons in segments located both within and outside the Hoxd11 expression domain (LS3-7, Landmesser, 1978; Hollyday, 1980). In the transfected sides of Hoxd11-electroporated embryos, ventral shank pools were normally positioned on the rostrocaudal axis with no indication of a rostral extension (Figs. 6E-F, n=7). These pools contained a few EGFP+, dextran+ motoneurons at the medial edge of the dextran+ pool but, as seen above, most EGFP+ motoneurons occupied a more medial position (Fig. 6G). In contrast, in control embryos (transfected with HB9 driven EGFP alone), EGFP+ motoneurons were often more laterally positioned and contributed in greater numbers to ventral shank pools (n=3, Fig. 6H).

In sum, the above data implicate Hoxd11 in specifying characteristics unique to a caudal LS subdomain. However, we were surprised to find so few EGFP+ motoneurons projecting to the ventral shank or caudilioflexorius muscle. We think it unlikely that most EGFP+ axons were projecting to other limb muscles because dextran injections at other sites also yielded low numbers or a complete absence of EGFP+, dextran+ cells (n=4 injections of full dorsal + ventral thigh and shank musculature; n=3 injections of the adductors of the ventral thigh; n=4 injections of the iliofibularis of the dorsal thigh; n=4 injections of the ischioflexorius of the ventral thigh).

To address this issue further, we examined the peripheral course of EGFP+ axons in a subset of Hb9::d11 embryos at stages 26-27 (n=6) and stage 29 (n=6). EGFP distribution was examined either in whole mount at the time of sacrifice or in sections stained additionally with anti-neurofilament. EGFP+ axons made substantial contributions to major limb nerve trunks (Fig. 6I-K) and to axial nerves. However, the distal extent of EGFP+ axons was often less than that of non-transfected, neurofilament+ axons (Fig. 6K). Further, despite the fact that assessments of LIM profiles indicated a reduction in Lim1+ (LMCl) motoneurons, no qualitative difference was evident in the distribution of EGFP+ axons to dorsal vs. ventral nerve trunks (see Fig. 6J). These observations suggest that axon outgrowth from many transfected motoneurons was delayed and/or that these axons were unable to detect and respond appropriately to peripheral guidance cues.

Two additional observations support the notions of abnormal axon-target interactions and a potential developmental delay. The ETS transcription factor, Pea3, is normally expressed in caudilioflexorius motoneurons in response to peripheral signals (Lin et al., 1998). While Pea3 +, EGFP+ motoneurons were occasionally found in Hb9::d11 embryos (Fig. 6L), they were very rare (approximately 1-3 cells per embryo, n=6 embryos). Thus, despite our observations of novel projections to the caudilioflexorius, it would appear that, in most cases, peripheral interactions were not sufficient to induce Pea3 expression. The guidance molecule, Slit2, is normally expressed widely by early differentiating motoneurons but becomes restricted to motoneuron subsets by stage 29 (Holmes and Niswander, 2001; Holmes et al., 1998; Lance-Jones, personal observations). We chose to examine Slit2 expression in LS sections from a subset of stage 29 Hb9::d11 embryos because of studies implicating Slit-robo signaling in both neuronal migration and motoneuron pathfinding (Geisen et al., 2008; Hammond et al., 2005).

In these embryos (n=7), Slit2 expression was noticeably higher than normal in regions corresponding to the position of most transfected cells (Fig. 6M-N), suggesting an arrest in maturation and a possible molecular correlate to the medial bias of transfected motoneurons.

In Hoxd11 transfected segments, motoneurons demonstrate a molecular profile suggestive of a suppression of LMC differentiation

Our finding of a marked decrease in LMCl motoneurons with ectopic Hoxd11 expression in rostral LS segments, coupled with the rostral extension of the caudilioflexorius pool, suggest a caudalization of segment identity. However, the abnormalities in motoneuron position and projections described above prompted us to characterize the molecular profiles of motoneurons within transfected segments in greater detail.

We show herein that misexpression of Hoxd11 in rostral LS segments increases the proportion of motoneurons expressing the LIM transcription factor Isl1. This marker is normally expressed by all newly generated motoneurons but maintained only in mature LMCm and MMC motoneurons (Tsuchida et al., 1994; Pfaff et al., 1996). To differentiate between LMCm and MMC, we examined expression of Foxp1 and the LIM transcription factor Lim3, which have recently been shown to act in opposition to one another to direct motoneurons towards an LMC or MMCm fate, respectively (Rousso et al., 2008; Dasen et al., 2008). In stage 29 Hb9::d11 embryos, we noted a reduction in the number of Foxp1+, LMC motoneurons on the transfected side of the spinal cord (Fig. 7A-C), though some transfected cells did express Foxp1 (arrows in Fig. 7D). In contrast, Lim3+ cells appeared to be present in increased numbers and in a less clustered pattern than normal (Fig. 7F). Numerous EGFP+, Lim3+ cells were evident in individual sections (Fig. 7H) and counts of Lim3+ motoneurons (Lim3+, Isl1/2+ cells) indicated a small but significant increase on transfected vs. non-transfected sides (Fig. 7G). In sum, the data presented here suggest that (1) ectopic Hoxd11 increased the proportion of MMCm motoneurons at the expense of the LMC, and (2) settling patterns may have been altered. However, the size of the Lim3+ population increase was considerably smaller than the decrease in the Foxp1+ population, suggesting that some motoneurons took on an alternate fate.

Several investigators have recently discussed the existence of lateral MMC (MMCl) cells at limb-innervating levels (Luria and Laufer, 2007; Rousso et al., 2008; Dasen et al., 2008). These motoneurons express neither Foxp1 nor Lim3, but do express high levels of Isl1, and the POU transcription factor, Scip. In order to include this population in our analyses, we examined expression of Scip in a subset of stage 29 Hb9::d11 embryos. Prior studies (see Rousso et al., 2008) suggest that Scip is highly expressed by MMCl motoneurons, although it is not an exclusive marker. It may additionally be expressed at low levels by MMCm motoneurons, by a small, dispersed population of Foxp1+ LMCm motoneurons at all LS levels, and by a discrete dorsolateral pool of Foxp1+ LMCm motoneurons at caudal LS levels (Luria and Laufer, 2007; Rousso et al, 2008). Following electroporation with Hb9::d11, we observed an increase in the total number of Scip+ motoneurons in LS2 (Fig. 7I-K). We found no increase in Scip+/Foxp1+ motoneurons (Table 1), implying that the increase in Scip+ expression affected the MMC exclusively. Two observations suggest that this increase impacts MMCl motoneurons. Many Scip+ motoneurons expressed high levels of Isl1, as assessed through fluorescence intensity measurements following anti-Isl1(2) staining (Fig. 7I-K, bottom half of stacked graph). Furthermore, while most Scip+ transfected motoneurons coexpressed Lim3, some did not (arrows in Fig. 7L). Taken together, these observations suggest a specific increase in the MMCl. Interestingly, we also noted that caudal segments (LS7-8) normally possess an expanded population of MMC motoneurons (Fig. 7M-N).

In sum, these data suggest that ectopic Hoxd11 caudalizes the rostral LS cord in two ways: by instructing motoneurons to project to a caudal target (the caudilioflexorius), and by promoting

the development of the MMC at the expense of the LMC. The observed decrease in the size of the LMC (Foxp1+ population), however, continues to exceed increases in both MMC cell types (Scip+ and/or Lim3+), implying that some motoneurons failed to differentiate into a recognized, mature phenotype.

Finally, it should be noted that the transfected sides of stage 29 Hb9::d11 embryos appeared to show an increased number of Lim3+, Isl1(2)- cells within or just dorsal to the motor columns (see Fig. 7F). In normal embryos, V2a interneurons occupy a similar position, are Lim3+, Isl1(2)-and Chx10+, and arise from a progenitor domain neighboring that of motoneurons (see Ericson et al., 1997;Briscoe et al., 2000). To identify this population, we stained sections from stage 29 Hb9::d11 embryos with anti-Chx10 as well as anti-EGFP. A few Chx10+ cells were EGFP+, but the vast majority of Chx10+ cells were EGFP- (Fig. 7O). Counts of the latter revealed a small but significant increase on transfected vs. non-transfected sides of the cord (mean number of Chx10+, EGFP- cells per section=70±5 on transfected side, 54±2 on non-transfected side, n=4 embryos, 3 sections per embryo, p=0.003, Fig. 7P). These data raise the possibility of a non-cell autonomous effect of ectopic Hoxd11 on V2a interneurons; however, a detailed characterization of interneuron profiles at different stages will be needed to address this possibility further.

Ectopic Hoxd11 downregulates the expression of RALDH2

We next sought a mechanistic explanation for observed shifts in motoneuron subtype distribution in Hoxd10- and Hoxd11-electroporated embryos. Prior studies have suggested that motoneuron-derived retinoic acid (RA) plays a critical role in the establishment of the LMC and later, the LMCl (Solomin et al., 1998; Sockanathan and Jessell, 1998; Sockanathan et al., 2003; Ji et al., 2009), and have linked expression of the RA synthetic enzyme, retinaldehyde dehydrogenase 2 (RALDH2), with Hox function in brachial spinal regions (Dasen et al., 2003; Vermot et al., 2005). We therefore hypothesized that Hoxd10 and Hoxd11 may regulate subtype distribution through modulation of RALDH2 expression.

Because prior studies of motoneuron-derived RA focused primarily on brachial levels, we first assessed RALDH2 patterns in the normal LS cord. At stage 23-24, RALDH2 is expressed at all LS levels, but only by Isl1/2+ motoneurons that have reached definitive motor column regions (Figs. 8A-C). By stage 29, RALDH2 expression is limited to particular motoneuron groups and varies by segment (Figs. 8D-F). In LS2, RALDH2 expression is restricted to a lateral crescent-shaped cluster, corresponding positionally to the LMCl. In LS4, the domain of RALDH2 expression has shifted to medial regions and overlaps with the area of Isl1(2)^{high} cells (LMCm). Expression levels gradually taper in more caudal segments – by LS6 motoneuron RALDH2 is barely detectable.

To examine the effects of Hox misexpression on RALDH2, sections from mid-LS (LS3-4) segments of stage 23-24 Hb9::Hox and β-actin::Hox and stage 29 β-actin::Hox embryos were stained with antibodies targeting RALDH2 and Isl1(2). The mean pixel intensity of RALDH2 staining within motor regions was determined using NIH ImageJ. In order to correct for any differences in motor column size on transfected and non-transfected sides, regions containing high Isl1(2) expression were manually circumscribed and mean pixel intensity of RALDH2 staining determined for that region alone. The circumscribed area comprised the entire motor column at stage 23-24. In stage 29 sections, it corresponded to medial motor column regions (see Fig. 8E). We observed no significant change in RALDH2 expression following transfection with Hoxd10 constructs (Fig. 8H, L). In embryos transfected with Hoxd11 constructs, however, we noted a significant ($p<0.01$) decline in mean pixel intensity of RALDH2 staining on the transfected side of the cord (Fig. 8I, L). Furthermore, while Hoxd10-transfected motoneurons were often RALDH2+ in rostral LS segments, there was little if any overlap between EGFP and RALDH2 expression in Hoxd11-transfected segments (Fig. 8J,

K). These data reveal that ectopic Hoxd11 leads to a downregulation of the expression of RALDH2, and raise the possibility that endogenous Hoxd11 prevents or arrests formation of the LMC and LMCl in caudal segments by decreasing RALDH2, and as a consequence, the local concentration of RA.

Ectopic Hoxd11 downregulates expression of endogenous Hoxd10

Since prior studies suggest that cell fate specification can reflect interactions between Hox genes (see Manzanares et al., 2001; Dasen et al., 2003 and 2005; Tumpel et al., 2007), we asked if transfection with either Hoxd10 or Hoxd11 altered the expression of the other. Electroporation with Hoxd10 did not visibly alter the distribution of endogenous Hoxd11 protein (n=3, stage 24; data not shown) or *hoxd11* transcript (n=9, stages 27-29; data not shown). In contrast, ectopic Hoxd11 in anterior LS segments appeared to cell-autonomously repress expression of Hoxd10 protein (n=3 stage 24, n=6 stage 29; Fig. 9A-B) and to downregulate *hoxd10* transcript (n=2/3 stage 24, n=7/8 stages 27-29; Fig. 9C-D). Similar results were obtained from electroporations using either Hb9 or b-actin promoter-driven constructs. We initially observed that endogenous Hoxd10 expression normally tapers off in caudal LS segments as the motor columns form (see Fig. 1R); the above findings suggest a unidirectional repression mechanism by which Hoxd11 downregulates expression of Hoxd10 in these segments.

DISCUSSION

Numerous prior studies indicate that a network of Hox genes directs the diversification of motoneurons within the hindbrain and rostral spinal segments. Considerably less information is available on the roles of Hox genes expressed in the developing caudal spinal cord. Experiments presented here examine the functions of two caudally expressed Hox genes, Hoxd10 and Hoxd11, in defining motoneuron columnar and pool complement within hindlimb innervating segments.

Hoxd10 and the establishment of the lumbar LMC

Our data suggest that Hoxd10 is instrumental in two aspects of LS/lumbar organization: (1) establishing the rostral boundary of the LS/lumbar cord as defined by the appearance of LMC motoneurons and the disappearance of the visceral motoneurons characteristic of thoracic segments, and (2) specifically promoting the development of the LMCl in rostral LS/lumbar segments. Evidence for the first role comes from our analysis of Hoxd10 loss-of-function mouse mutants, which exhibit a caudal half-segment shift in the rostral boundary of the lumbar spinal cord (see also Carpenter et al., 1997), as well as studies where features characteristic of LS motoneurons are induced with ectopic Hoxd10 expression in chick thoracic segments (Shah et al., 2004; Dasen et al., 2008). Furthermore, Wu et al. (2008) recently reported that loss of both Hoxc10 and d10 expression in the spinal cord results in a multi-segment caudal shift in the thoraco-lumbar boundary. Our data specifically implicate Hoxd10 as a contributing factor to this phenomenon.

At early stages of motoneuron differentiation, Hoxd10 is expressed throughout the LS region of the spinal cord, suggesting an early, uniform role in LS development. Based on evidence presented above, one aspect of this early function may be the establishment of the LS as a whole, as defined by the presence of an LMC. As such, Hoxd10 shares features in common with Hoxc6, a Hox protein critical for the specification of the brachial LMC as a whole (Dasen et al., 2003). There are also parallels between the functions of Hox10 genes in neural and somatic mesoderm derivatives, as analyses of mice with knockouts of multiple Hox have led to the conclusion that Hox10 paralogues function as specifiers of lumbar vertebral identity (Wellik and Capecchi, 2003; Wellik, 2007).

Hoxd10 and the development of the LMCl

Evidence for the second proposed role of Hoxd10, the promotion of LMCl development in rostral LS/lumbar segments, comes from both loss- and gain-of-function studies. In chick, transient overexpression of Hoxd10 initiated in early postmitotic motoneurons results in an early increase in motoneurons with a LIM code characteristic of LMCl subtypes (Lim1+, Isl1-). Overexpression initiated at progenitor stages with β-actin-driven constructs and maintained through stages of motor column formation increases the proportion of motoneurons with the Lim1+ molecular phenotype, lateral position and dorsal axonal trajectory characteristic of LMCl motoneurons. These experiments also lead to a substantial decrease in motoneuron numbers. While a toxic effect on early born, future LMCm motoneurons could be suggested, the fact that related experiments with Hoxd11 show decreases in a different population (late born LMCm motoneurons) suggests that the effects of Hoxd10 misexpression are unique. Furthermore, in complementary fashion, Hoxd10 loss-of-function mouse mutants exhibit a marked decrease in LMCl motoneurons in rostral lumbar segments at stages just after motor column formation. These findings again parallel those of Wu and colleagues (2008), who describe a severe reduction in LMCl numbers in Hoxc10/Hoxd10 double knockout mice. However, they report no obvious change in subtype complement in single Hoxd10 knockout mice. This difference in outcome could reflect differences in the methods used to delete Hoxd10 function (see Wu et al., 2008), or the fact that quantification was necessary to see the reduction. Regardless, our findings strongly suggest a role for Hoxd10 in LMCl specification.

Data presented here also provide evidence relevant to the timing of Hoxd10 function in LMCl formation. In embryos electroporated with Hb9-driven Hoxd10 constructs, the increase in Lim1 + motoneurons found at stage 23-25 is not accompanied by a change in total motoneuron numbers (Isl1(2)+ cells) or a change in total LMC numbers (Foxp1+ cells), suggesting that Hoxd10 initiated a fate switch among early postmitotic motoneurons rather than a change in cell survival and a fate switch from LMCm to LMCl. These conclusions are compatible with prior studies indicating that the programming of LMCl vs. LMCm fate occurs shortly after motoneurons withdraw from the cell cycle (Sockanathan and Jessell, 1998). In these embryos, both Hoxd10 overexpression and the increase in Lim1+ motoneurons are transient, suggesting that Hoxd10 expression must be sustained at least through early stages of motor column formation to influence motoneuron phenotype and are compatible with prior studies suggesting that the early programming of the LMCl is labile (Sockanathan and Jessell, 1998). Rousso and colleagues (2008) noted a similar phenomenon in mutant mice lacking Foxp1, a transcription factor necessary for LMC development and closely linked by the same investigators to Hox10 function at LS/lumbar levels.

While overexpression of Hoxd10 has been shown here to increase the number or proportion of cells expressing the LMCl marker Lim1, it is important point out that this effect may not be direct. For example, since prior studies demonstrate cross-repressive interactions between Lim1 and Isl1 (Kania and Jessell, 2003), it is possible that Hoxd10 operates by limiting Isl1+ LMCm formation. A suppression of Isl1 expression may also explain the rapid downregulation of Hoxd10 under the Hb9 promoter, as Isl1 binds directly to the Hb9 promoter (Lee and Pfaff, 2003) and is required for endogenous Hb9 expression in motoneurons (Pfaff et al., 1996). Hb9::d10 may, therefore, feed back to repress its own expression via downregulation of Isl1.

During the period of motor column formation, the widespread initial expression of Hoxd10 within motoneuron populations narrows, such that by stage 29, expression is largely limited to subsets of motoneurons in LS1-5. In the most rostral of these segments (LS1-2), expression is restricted to Lim1+, LMCl motoneurons that occupy a position corresponding to that of motor pools projecting to two prominent dorsal thigh muscles, the sartorius and anterior iliotibialis (Landmesser, 1978). Our analyses of motoneuron subtype complement in Hoxd10 mutants indicate a loss of LMCl motoneurons that is greatest in rostral segments and likely to

include the homologous motor pools. Further, Hoxa10+/-, Hoxc10-/-, Hoxd10-/- mutants show a pronounced loss of Foxp1 that is greatest in rostral lumbar segments (Rousso et al., 2008). Since our findings also suggest that the early programming of a Lim1+ LMCl phenotype is labile, it is possible that long-term, sustained Hoxd10 expression in rostral segments is critical for the development of this feature of a rostral LS segment identity.

While our data strongly support the hypothesis that Hoxd10 promotes the normal development of a large complement of LMCl motoneurons in rostral LS segments, two observations merit attention. First, our Hoxd10 manipulations in both mice and chick systems elicited changes in LMCl numbers that are relatively small (approximately 10-20% decreases or increases). In contrast, much more dramatic changes in LMCl motoneurons are found in Hoxc10/Hoxd10 double knockout mice (Wu et al. 2008). These observations are most compatible with the hypothesis that Hoxd10 and Hoxc10 coordinately regulate motoneuron subtype development. Analyses of the position of the LMC in different mouse mutants also suggest the involvement of multiple Hox10 proteins in establishing the thoracic-lumbar border. Our counts of LMCl, LMCm and MMC numbers in Hoxd10 mutant embryos suggest a 1/2 segment caudal shift in lumbar LMC position, a conclusion similar to that reached by Carpenter et al. (1997) on the basis of morphological criteria in neonates. In contrast, 2-3 segment shifts are described for Hoxd10/Hoxc10 (Wu et al. 2008) and Hoxa10/Hoxd10 (Lin and Carpenter, 2003) double mutants. As for the somite-derived vertebral skeleton (Wellik and Capecchi, 2003), functional redundancy and cooperativity appear to exist. An elucidation of the independent functions of Hoxc10 would be of considerable interest, given that Hoxc proteins figure prominently in the development of motoneuron identity in brachial segments (Dasen et al., 2005).

The second point to be made is that there is not a simple link between the maintenance of either Hoxd10 expression and the development a Lim1+, LMCl phenotype in all LS segments. In middle LS segments (i.e. LS3-4) in the stage 29 chick embryo, Hoxd10 is expressed not by LMCl motoneurons, but by LMCm motoneurons that project to ventral shank muscles (data presented here and personal observations). Despite the fact that Foxp1 appears to be a broad marker of LMC motoneurons (Dasen et al., 2008; Rousso et al., 2008), we also find that normal Foxp1 expression levels are low in some subsets of LMCm motoneurons in LS3-4 (Misra, preliminary observations). Our current studies do not indicate a likely function for these patterns, but do suggest that different hierarchies of transcription factors mold motor pools in rostral and middle LS segments.

Hoxd11 and the development of a caudal LS identity

The specific role of Hoxd11 in motoneuron development has not been addressed prior to this study. Evidence presented here from gain-of-function experiments reveals that Hoxd11 plays a dual role in the establishment of caudal LS motoneuron identity by: (1) specifying caudal motor pools, and (2) shifting, via direct or indirect repression of other factors, overall motoneuron complement toward medial phenotypes. Evidence for the first role is derived primarily from retrograde labeling experiments. We show that misexpression of Hoxd11 in rostral and middle LS segments is sufficient to induce ectopic axonal projections from these segments to a caudal limb muscle, the caudilioflexorius. Our observations complement studies by Dasen and colleagues (2005) in the brachial spinal cord. These investigators noted that expansion of the expression of Hoxc8 from caudal brachial segments into more rostral segments induced a small number of rostral motoneurons to send novel axonal projections to a caudal muscle target, the pectoralis.

Evidence suggesting a second, more general role for Hoxd11 in columnar regulation comes from gain-of-function experiments in which molecular profiles as well as projection patterns of transfected motoneurons were examined. We first observed that Hoxd11 misexpression in rostral LS segments leads to disproportionate decreases in the size of the LMCl, as defined by

expression of Lim1. These decreases are accompanied by increases in the expression of markers of more medial motoneuron subtypes, including Isl1, which designates both LMCm and MMC motoneurons, and Lim3 and Scip, which primarily designate MMC motoneurons. Increased expression of MMC markers was in turn accompanied by a loss of the LMC marker, Foxp1. In a normal embryo, Hoxd11 expression is restricted to caudal LS segments where the population of Lim1+, dorsal-projecting LMCl motoneurons is small and the MMC population expanded. Our findings are broadly compatible with the hypothesis that ectopic Hoxd11 initiates a "caudalization" or phenotypic conversion of rostral LS segments to a more caudal LS identity. Hoxd11 manipulation leads to related phenotypic conversions of the axial skeleton (Davis and Capecchi, 1994; Zakany et al, 1996; Boulet and Capecchi, 2002). Hoxd11 over-expressing mice exhibit a reduction in the number of lumbar vertebrae (Boulet and Cappechi, 2002). Conversely, Hoxd11 loss-of-function mutants exhibit a one-segment gain in lumbar vertebrae at the expense of sacral vertebrae (Davis and Capecchi, 1994; Wellik and Capecchi, 2003). Thus, Hoxd11 may function in the regulation of lumbar/LS size and the specification of "sacral" or caudal LS identity in both neural and mesodermal tissues.

Hoxd11 and motor column maturation

Two additional features characterize rostral segments with ectopic Hoxd11 expression. First, the clustering of motoneurons appears to be altered. Hoxd11-transfected cells showed both a medial bias and a tendency to be less tightly clustered than normal. Hox genes have been implicated in neuronal migration (Goddard et al., 1996; Studer et al., 1996; Cooper et al., 2003; Holstege et al., 2008; Geisen et al., 2008) and several adhesion/guidance molecules figure among the downstream effectors of Hox function (see Akin and Nazarali, 2005; Pearson et al., 2005; Svingen and Tonissen, 2006, Geisen et al., 2008). In Hoxd11 transfected cords, we find changes in the expression of Slit 2, a molecule highly expressed by developing spinal motoneurons (Holmes and Niswander, 2001) and demonstrably involved in neuronal migration (see Geisen et al., 2008) and motor axon pathfinding (see Hammond et al., 2005). While numerous other guidance molecules and signaling systems might also be altered, this observation focuses attention on slit-robo signaling components as potential downstream targets for caudally-expressed Hox.

The extreme medial location of transfected motoneurons and the molecular profiles of cells within transfected motor columns suggest a second feature initiated by Hoxd11 expression, that is, an arrest of motoneuron differentiation and maturation. Isl1, Lim3, Scip, and Slit2 are factors normally expressed by all motoneurons immediately following birth and subsequently downregulated in specific mature motoneuron subtypes (Ericson et al., 1992; Pfaff et al., 1996; Sharma et al., 1998 and 2000; Holmes et al., 1998). As noted above, we observed increases in expression of all of these factors and a concomitant decrease in expression of the mature LMC marker Foxp1 (Dasen et al, 2008; Rousso et al., 2008). Such shifts in molecular profile may point toward an overall shift in columnar distribution toward medial subtypes, or may reflect a failure of transfected motoneurons to mature beyond the initial stages of motoneuron development. Indeed, immaturity may explain the apparent incongruity between a severe loss of Foxp1+ LMC motoneurons and minor gains in Scip+ and/or Lim3+ MMC motoneurons in Hoxd11-transfected embryos, as high levels of Hoxd11 expression may have left an immature population of motoneurons expressing markers of neither LMC nor MMC. Our findings of aberrant and shortened axonal projections in the limb and only a small number of transfected cells contributing to motor pools are also compatible with this hypothesis. Below we discuss two interconnected mechanisms by which Hoxd11 may repress the development and maturation of the LMC.

Hoxd10-d11 interactions and regulation of RA signaling

Repressive interactions among Hox genes have long been described as a driving force in segmental diversification (see Duboule and Morata, 1994, Dasen et al., 2005). We show here that ectopic Hoxd11 is sufficient to cell-autonomously repress endogenous Hoxd10 transcript and protein expression in rostral lumbar segments. These findings parallel studies in which unidirectional repression of Hoxc5 by Hoxc8 was shown to play a role in the definition of subdomains within the brachial cord (Dasen et al., 2005) as well as studies implicating cross-talk between Hox genes during hindbrain development (see Tumpel et al., 2007). Such a mechanism may be responsible for the decline in Hoxd10 expression seen in caudal LS segments during normal motor column formation. When coupled with the above conclusion that Hoxd10 is necessary for the establishment of the LMC as a whole and capable of inducing the expression of Lim1+, a critical determinant of LMCl identity, repression of Hoxd10 by Hoxd11 suggests a cell-autonomous mechanism by which endogenous Hoxd11 regulates subtype complement in caudal LS segments. It may also explain the existence of motoneurons that seemingly belong to neither LMC nor MMC populations, as Wu et al. (2008) have shown that Hoxc10/d10 loss-of-function mutants possess motoneurons that do not adopt or maintain markers of either group.

Recent studies (Dasen et al., 2008; Rousso et al., 2008) suggest that Hoxd10 as well as other Hox10 paralogues induce Foxp1. The phenotype we observed following Hoxd11 overexpression closely parallels that of Foxp1 loss-of-function mouse mutants (Dasen et al., 2008; Rousso et al., 2008). Foxp1 mutants exhibit an overall decrease in the size of the LMC, and an increase in the size of the Lim3+ and Scip+ MMC populations. Furthermore, they show a specific loss of Lim1+ motoneurons and aberrant axonal projections to limb targets. Such close parallels implicate Foxp1 as a downstream target of Hoxd11-mediated regulation either directly or via suppression of Hoxd10 expression.

Expression of the RA synthetic enzyme RALDH2 is a defining characteristic of limb-innervating spinal regions, and it has been shown to be necessary for motoneuron survival, maturation of the LMC, and induction of the LMCl marker Lim1 (Sockanathan and Jessell, 1998; Sockanathan et al., 2003; Vermot et al., 2005; Ji et al., 2006). Loss of RALDH2 results in a decrease in LMC motoneurons (LMCl in particular), atrophy of limb-innervating motoneurons and/or their axon projections, and mispositioning of motor pools (Vermot et al., 2005; Ji et al., 2006). Local RA levels can therefore significantly impact motoneuron subtype proportions and maturation.

At stages of LMCl/LMCm differentiation (stages 23-24) as well as stages just after normal motor column formation (stage 29), we find small but significant decreases in RALDH2 expression with ectopic Hoxd11 expression. These decreases in the rostral LS may parallel endogenous RALDH2 decreases in caudal LS segments during normal motor column formation, where Hoxd11 is present at high concentrations and the LMCl is very small. Given the positive associations among RA signaling, LMC development, and LMCl specification, downregulation of local RA levels may serve as a non-cell-autonomous mechanism for the regulation of motoneuron distribution by Hoxd11 in caudal LS segments. Indeed, mice lacking functional motoneuron-derived RALDH2 (Vermot et al., 2005) demonstrate many of the same characteristics as our Hoxd11 overexpression model, including a decrease in overall motoneuron number, a disproportionate loss of Lim1+ motoneurons, and the premature halt of distal axon growth in the periphery. These mutants, however, exhibit no alterations in MMC distribution, suggesting that Hoxd11 may also be acting via other mechanisms.

Our studies do not answer the question of whether Hoxd11 directly suppresses RALDH2 expression or whether the former is a consequence of lowered Hoxd10 and/or Foxp1. Ectopic Hoxd10 expression in the thoracic neural tube induces ectopic RALDH2 expression (Shah et

al., 2004) while the loss of Hoxd10 or Foxp1 decreases RALDH2 (Wu et al., 2008; Dasen et al., 2008). We show here that normal RALDH2 expression patterns within the LS cord parallel those of Hoxd10; both are expressed widely in the LS LMC at early stages of motor column formation and become restricted to subsets of motoneurons in LS1-5, including Lim1+, LMCl motoneurons in LS1-2. Given these observations, we were surprised to find no evidence of an increase in RALDH2 levels with Hoxd10 overexpression. Our method of RALDH2 quantification may have lacked the sensitivity to detect subtle increases in expression levels, especially if cellular processes on transfected cells were reduced, or the high levels of Hoxd10 induced by electroporation may have activated a negative feedback. However, it is also possible that Hoxd10 promotes the development of an LS LMCl phenotype in rostral segments via a RALDH2-independent mechanism. Our observation that the proportion of Lim1+ cells among the transfected population in st 24 Hb9::d10 embryos was higher than the proportion of Lim1 + cells in the motor columns as a whole raise the possibility of cell-autonomous function. Since Hox transcriptional targets include RA receptors (Serpente et al., 2005; Rohrschneider et al., 2007), a hypothesis to be considered in the future is that Hoxd10 regulates RA receptors in a cell-autonomous manner in developing LS motoneurons.

Our experiments also provide preliminary evidence that ectopic Hoxd11 affects interneuron numbers. In stage 29 Hb9:d11 embryos, Chx10+ V2a interneuron numbers in LS segments were increased by approximately 30% on transfected sides when compared to non-transfected sides. The cells counted at stage 29 were EGFP-, suggesting that they had not been transfected. However, the question of just what non-cell autonomous and/or cell autonomous events underlie these findings awaits analyses of molecular profiles at additional stages in normal and experimental embryos. Recent analyses of mice lacking neuronal Chx10 expression define a role for Chx10+ V2a interneurons in locomotor coordination and indicate that V2a interneurons express Hox10 paralogues (Crone et al., 2008). These observations raise the questions of whether our findings reflect intracellular interactions between ectopic Hoxd11 and endogenous Hox10 proteins and/or whether early intercellular interactions between circuit neurons could be regulating neuronal number. Future studies might also ask if RA levels influence the development of Chx10+ cells, given extant evidence of retinoic acid activity in ventral spinal regions including interneurons (see Shiga et al., 1995; Solomin et al., 1998; Pierani et al., 1999; Niederreither et al., 2002; Wilson et al., 2004) and our finding of decreased RALDH2 levels with ectopic Hoxd11 expression.

Independent of any influence on interneurons, our data, in sum, suggest that interactions between Hoxd11 and Hoxd10 influence the distribution of motoneuron subtypes along the rostrocaudal axis (Fig. 9E). Hoxd10 appears to define the rostral boundaries of the LS LMC, to direct LMC maturation, and to promote the development of features specific to the rostral LS, such as a large LMCl. Hoxd11 appears to function as a specifier of at least one caudal motor pool but also acts in caudal LS segments to dampen the effects of Hoxd10 and potentially also RALDH2. We would suggest that our results with ectopic Hoxd11 expression represent an exaggerated version of a normal dampening responsible for the development of additional caudal LS features, including a diminishing LMC, and a relatively larger population of medial motoneuron subtypes.

Acknowledgments

The authors thank Laura Lillien for critical comments on the data and their interpretation, Paula Monaghan-Nichols, for help with DNA construct preparation, and Emily Sours for excellent technical assistance. We also thank Tom Jessell, Cathy Krull, Sam Pfaff, Cliff Tabin, Jonathan Raper and the Developmental Studies Hybridoma Bank (University of Iowa) for providing reagents. This work was funded by NIH grants to C.L.-J. (R01-HD025676) and M.M. (T32-NS007433-07).

References

Akin ZN, Nazarali AJ. Hox genes and their candidate downstream targets in the developing central nervous system. Cell Mol Neurobiol 2005;25:697–741. [PubMed: 16075387]

Arber S, et al. Requirement for the homeobox gene Hb9 in the consolidation of motor neuron identity. Neuron 1999;23:659–74. [PubMed: 10482234]

Boulet AM, Capecchi MR. Duplication of the Hoxd11 gene causes alterations in the axial and appendicular skeleton of the mouse. Dev Biol 2002;249:96–107. [PubMed: 12217321]

Briscoe J, et al. A homeodomain protein code specifies progenitor cell identity and neuronal fate in the ventral neural tube. Cell 2000;101:435–45. [PubMed: 10830170]

Briscoe J, Wilkinson DG. Establishing neuronal circuitry: Hox genes make the connection. Genes Dev 2004;18:1643–8. [PubMed: 15256497]

Carpenter EM, et al. Targeted disruption of Hoxd-10 affects mouse hindlimb development. Development 1997;124:4505–14. [PubMed: 9409668]

Cooper KL, et al. Autonomous and nonautonomous functions for Hox/Pbx in branchiomotor neuron development. Dev Biol 2003;253:200–13. [PubMed: 12645925]

Crone SA, et al. Genetic ablation of V2a ipsilateral interneurons disrupts left-right locomotor coordination in mammalian spinal cord. Neuron 2008;60:70–83. [PubMed: 18940589]

Dasen JS, et al. Hox repertoires for motor neuron diversity and connectivity gated by a single accessory factor, FoxP1. Cell 2008;134:304–16. [PubMed: 18662545]

Dasen JS, et al. Motor neuron columnar fate imposed by sequential phases of Hox-c activity. Nature 2003;425:926–33. [PubMed: 14586461]

Dasen JS, et al. A Hox regulatory network establishes motor neuron pool identity and target-muscle connectivity. Cell 2005;123:477–91. [PubMed: 16269338]

Davis AP, Capecchi MR. Axial homeosis and appendicular skeleton defects in mice with a targeted disruption of hoxd-11. Development 1994;120:2187–98. [PubMed: 7925020]

de la Cruz CC, et al. Targeted disruption of Hoxd9 and Hoxd10 alters locomotor behavior, vertebral identity, and peripheral nervous system development. Dev Biol 1999;216:595–610. [PubMed: 10642795]

De Marco Garcia NV, Jessell TM. Early motor neuron pool identity and muscle nerve trajectory defined by postmitotic restrictions in Nkx6.1 activity. Neuron 2008;57:217–31. [PubMed: 18215620]

di Sanguinetto SA, et al. Transcriptional mechanisms controlling motor neuron diversity and connectivity. Curr Opin Neurobiol 2008;18:36–43. [PubMed: 18524570]

Dolle P, Duboule D. Two gene members of the murine HOX-5 complex show regional and cell-type specific expression in developing limbs and gonads. Embo J 1989;8:1507–15. [PubMed: 2569970]

Duboule D, Morata G. Colinearity and functional hierarchy among genes of the homeotic complexes. Trends Genet 1994;10:358–64. [PubMed: 7985240]

Eberhart J, et al. EphA4 constitutes a population-specific guidance cue for motor neurons. Dev Biol 2002;247:89–101. [PubMed: 12074554]

Eisen JS. Patterning motoneurons in the vertebrate nervous system. Trends Neurosci 1999;22:321–6. [PubMed: 10370257]

Ensini M, et al. The control of rostrocaudal pattern in the developing spinal cord: specification of motor neuron subtype identity is initiated by signals from paraxial mesoderm. Development 1998;125:969–82. [PubMed: 9463344]

Ericson J, et al. Pax6 controls progenitor cell identity and neuronal fate in response to graded Shh signaling. Cell 1997;90:169–80. [PubMed: 9230312]

Ericson J, et al. Early stages of motor neuron differentiation revealed by expression of homeobox gene Islet-1. Science 1992;256:1555–60. [PubMed: 1350865]

Geisen MJ, et al. Hox paralog group 2 genes control the migration of mouse pontine neurons through slit-robo signaling. PLoS Biol 2008;6:e142. [PubMed: 18547144]

Goddard JM, et al. Mice with targeted disruption of Hoxb-1 fail to form the motor nucleus of the VIIth nerve. Development 1996;122:3217–28. [PubMed: 8898234]

Guthrie S. Patterning and axon guidance of cranial motor neurons. Nat Rev Neurosci 2007;8:859–71. [PubMed: 17948031]

Hamburger V, Hamilton HL. A series of normal stages in the development of the chick embryo. J Morphol 1951;88:49–92.

Hamburger V, Oppenheim RW. Naturally occurring neuronal death in vertebrates. Neuroscience Commentaries 1982;1:39–55.

Hammond R, et al. Slit-mediated repulsion is a key regulator of motor axon pathfinding in the hindbrain. Development 2005;132:4483–95. [PubMed: 16162649]

Hollyday M. Organization of motor pools in the chick lumbar lateral motor column. J Comp Neurol 1980;194:143–70. [PubMed: 7192292]

Hollyday M, Hamburger V. An autoradiographic study of the formation of the lateral motor column in the chick embryo. Brain Res 1977;132:197–208. [PubMed: 890480]

Holmes G, Niswander L. Expression of slit-2 and slit-3 during chick development. Dev Dyn 2001;222:301–7. [PubMed: 11668607]

Holmes GP, et al. Distinct but overlapping expression patterns of two vertebrate slit homologs implies functional roles in CNS development and organogenesis. Mech Dev 1998;79:57–72. [PubMed: 10349621]

Holstege JC, et al. Loss of Hoxb8 alters spinal dorsal laminae and sensory responses in mice. Proc Natl Acad Sci U S A 2008;105:6338–43. [PubMed: 18430798]

Hutchinson SA, Eisen JS. Islet1 and Islet2 have equivalent abilities to promote motoneuron formation and to specify motoneuron subtype identity. Development 2006;133:2137–47. [PubMed: 16672347]

Jessell TM. Neuronal specification in the spinal cord: inductive signals and transcriptional codes. Nat Rev Genet 2000;1:20–9. [PubMed: 11262869]

Ji SJ, et al. Nolz1 is induced by retinoid signals and controls motoneuron subtype identity through distinct repressor activities. Development 2009;136:231–40. [PubMed: 19056829]

Ji SJ, et al. Mesodermal and neuronal retinoids regulate the induction and maintenance of limb innervating spinal motor neurons. Dev Biol 2006;297:249–61. [PubMed: 16781703]

Kania A, Jessell TM. Topographic motor projections in the limb imposed by LIM homeodomain protein regulation of ephrin-A:EphA interactions. Neuron 2003;38:581–96. [PubMed: 12765610]

Kania A, et al. Coordinate roles for LIM homeobox genes in directing the dorsoventral trajectory of motor axons in the vertebrate limb. Cell 2000;102:161–73. [PubMed: 10943837]

Lance-Jones C. Motoneuron cell death in the developing lumbar spinal cord of the mouse. Brain Res 1982;256:473–9. [PubMed: 7127154]

Lance-Jones C. Patterns of motoneuron projections in the embryonic mouse hindlimb prior to cell death. Society for Neuroscience Abstracts 1984;10:639.

Lance-Jones C, et al. *Hoxd10* induction and regionalization in the developing lumbosacral spinal cord. Development 2001;128:2255–2268. [PubMed: 11493545]

Landmesser L. The distribution of motoneurones supplying chick hind limb muscles. J Physiol 1978;284:371–89. [PubMed: 731549]

Landmesser LT. The acquisition of motoneuron subtype identity and motor circuit formation. Int J Dev Neurosci 2001;19:175–82. [PubMed: 11255031]

Lee SK, Pfaff SL. Synchronization of neurogenesis and motor neuron specification by direct coupling of bHLH and homeodomain transcription factors. Neuron 2003;38:731–45. [PubMed: 12797958]

Lin AW, Carpenter EM. Hoxa10 and Hoxd10 coordinately regulate lumbar motor neuron patterning. J Neurobiol 2003;56:328–37. [PubMed: 12918017]

Lin JH, et al. Functionally related motor neuron pool and muscle sensory afferent subtypes defined by coordinate ETS gene expression. Cell 1998;95:393–407. [PubMed: 9814709]

Liu JP, et al. Assigning the Positional Identity of Spinal Motor Neurons. Rostrocaudal Patterning of Hox-c Expression by FGFs, Gdf11, and Retinoids Neuron 2001;32:997–1012.

Livet J, et al. ETS gene Pea3 controls the central position and terminal arborization of specific motor neuron pools. Neuron 2002;35:877–92. [PubMed: 12372283]

Lumsden A, Krumlauf R. Patterning the vertebrate neuraxis. Science 1996;274:1109–15. [PubMed: 8895453]

Luria V, Laufer E. Lateral motor column axons execute a ternary trajectory choice between limb and body tissues. Neural Develop 2007;2:13.

Manzanares M, et al. Independent regulation of initiation and maintenance phases of Hoxa3 expression in the vertebrate hindbrain involve auto- and cross-regulatory mechanisms. Development 2001;128:3595–607. [PubMed: 11566863]

Matise MP, Lance-Jones C. A critical period for the specification of motor pools in the chick lumbosacral spinal cord. Development 1996;122:659–69. [PubMed: 8625817]

Misra, M.; Lance-Jones, C. Society for Neuroscience, Vol. Program No. 23.18. Washington, DC: 2008. A role for Hox D11 in posterior lumbosacral motoneuron specification in the spinal cord of the chick embryo.

Misra, M., et al. Society for Neuroscience, Vol. Program No. 596.15. Washington, DC: 2005. Evidence that Hoxd10 and Hoxd11 have different roles in the development of lateral and medial motoneuron subtypes in the spinal cord of the chick embryo.

Niederreither K, et al. Retinaldehyde dehydrogenase 2 (RALDH2)- independent patterns of retinoic acid synthesis in the mouse embryo. Proc Natl Acad Sci U S A 2002;99:16111–6. [PubMed: 12454286]

Nieto MA, et al. In situ hybridization analysis of chick embryos in whole mount and tissue sections. Methods Cell Biol 1996;51:219–35. [PubMed: 8722478]

Pearson JC, et al. Modulating Hox gene functions during animal body patterning. Nat Rev Genet 2005;6:893–904. [PubMed: 16341070]

Pfaff SL, et al. Requirement for LIM homeobox gene Isl1 in motor neuron generation reveals a motor neuron-dependent step in interneuron differentiation. Cell 1996;84:309–20. [PubMed: 8565076]

Pierani A, et al. A sonic hedgehog-independent, retinoid-activated pathway of neurogenesis in the ventral spinal cord. Cell 1999;97:903–15. [PubMed: 10399918]

Rijli FM, et al. Cryptorchidism and homeotic transformations of spinal nerves and vertebrae in Hoxa-10 mutant mice. Proc Natl Acad Sci U S A 1995;92:8185–9. [PubMed: 7667266]

Rohrschneider MR, et al. Zebrafish Hoxb1a regulates multiple downstream genes including prickle1b. Dev Biol 2007;309:358–72. [PubMed: 17651720]

Rousso DL, et al. Coordinated actions of the forkhead protein Foxp1 and Hox proteins in the columnar organization of spinal motor neurons. Neuron 2008;59:226–40. [PubMed: 18667151]

Schaeren-Wiemers N, Gerfin-Moser A. A single protocol to detect transcripts of various types and expression levels in neural tissue and cultured cells: in situ hybridization using digoxigenin-labelled cRNA probes. Histochemistry 1993;100:431–40. [PubMed: 7512949]

Serpente P, et al. Direct crossregulation between retinoic acid receptor {beta} and Hox genes during hindbrain segmentation. Development 2005;132:503–13. [PubMed: 15634700]

Shah V, et al. Ectopic expression of Hoxd10 in thoracic spinal segments induces motoneurons with a lumbosacral molecular profile and axon projections to the limb. Dev Dyn 2004;231:43–56. [PubMed: 15305286]

Sharma K, et al. Genetic and epigenetic mechanisms contribute to motor neuron pathfinding. Nature 2000;406:515–9. [PubMed: 10952312]

Sharma K, et al. LIM homeodomain factors Lhx3 and Lhx4 assign subtype identities for motor neurons. Cell 1998;95:817–28. [PubMed: 9865699]

Shiga T, et al. The development of interneurons in the chick embryo spinal cord following in vivo treatment with retinoic acid. J Comp Neurol 1995;360:463–74. [PubMed: 8543652]

Shirasaki R, et al. FGF as a target-derived chemoattractant for developing motor axons genetically programmed by the LIM code. Neuron 2006;50:841–53. [PubMed: 16772167]

Shirasaki R, Pfaff SL. Transcriptional codes and the control of neuronal identity. Annu Rev Neurosci 2002;25:251–81. [PubMed: 12052910]

Sockanathan S, Jessell TM. Motor neuron-derived retinoid signaling specifies the subtype identity of spinal motor neurons. Cell 1998;94:503–14. [PubMed: 9727493]

Sockanathan S, et al. Retinoid receptor signaling in postmitotic motor neurons regulates rostrocaudal positional identity and axonal projection pattern. Neuron 2003;40:97–111. [PubMed: 14527436]

Solomin L, et al. Retinoid-X receptor signalling in the developing spinal cord. Nature 1998;395:398–402. [PubMed: 9759732]

Studer M, et al. Altered segmental identity and abnormal migration of motor neurons in mice lacking Hoxb-1. Nature 1996;384:630–4. [PubMed: 8967950]

Svingen T, Tonissen KF. Hox transcription factors and their elusive mammalian gene targets. Heredity 2006;97:88–96. [PubMed: 16721389]

Tanabe Y, et al. Specification of motor neuron identity by the MNR2 homeodomain protein. Cell 1998;95:67–80. [PubMed: 9778248]

Tarchini B, et al. HoxD cluster scanning deletions identify multiple defects leading to paralysis in the mouse mutant Ironside. Genes Dev 2005;19:2862–76. [PubMed: 16322559]

Thaler J, et al. Active suppression of interneuron programs within developing motor neurons revealed by analysis of homeodomain factor HB9. Neuron 1999;23:675–87. [PubMed: 10482235]

Thaler JP, et al. A postmitotic role for Isl-class LIM homeodomain proteins in the assignment of visceral spinal motor neuron identity. Neuron 2004;41:337–50. [PubMed: 14766174]

Tiret L, et al. Increased apoptosis of motoneurons and altered somatotopic maps in the brachial spinal cord of Hoxc-8-deficient mice. Development 1998;125:279–91. [PubMed: 9486801]

Tsuchida T, et al. Topographic organization of embryonic motor neurons defined by expression of LIM homeobox genes. Cell 1994;79:957–70. [PubMed: 7528105]see comments

Tumpel S, et al. Expression of Hoxa2 in rhombomere 4 is regulated by a conserved cross-regulatory mechanism dependent upon Hoxb1. Dev Biol 2007;302:646–60. [PubMed: 17113575]

Vermot J, et al. Retinaldehyde dehydrogenase 2 and Hoxc8 are required in the murine brachial spinal cord for the specification of Lim1+ motoneurons and the correct distribution of Islet1+ motoneurons. Development 2005;132:1611–21. [PubMed: 15753214]

Wahba GM, et al. The paralogous Hox genes Hoxa10 and Hoxd10 interact to pattern the mouse hindlimb peripheral nervous system and skeleton. Dev Biol 2001;231:87–102. [PubMed: 11180954]

Wellik DM. Hox patterning of the vertebrate axial skeleton. Dev Dyn 2007;236:2454–63. [PubMed: 17685480]

Wellik DM, Capecchi MR. Hox10 and Hox11 genes are required to globally pattern the mammalian skeleton. Science 2003;301:363–7. [PubMed: 12869760]

William CM, et al. Regulation of motor neuron subtype identity by repressor activity of Mnx class homeodomain proteins. Development 2003;130:1523–36. [PubMed: 12620979]

Wilson L, et al. Retinoic acid and the control of dorsoventral patterning in the avian spinal cord. Dev Biol 2004;269:433–46. [PubMed: 15110711]

Wu Y, et al. Hoxc10 and Hoxd10 regulate mouse columnar, divisional and motor pool identity of lumbar motoneurons. Development 2008;135:171–82. [PubMed: 18065432]

Yip JW, et al. Specific projections of sympathetic preganglionic neurons are not intrinsically determined by segmental origins of their cell bodies. J Neurobiol 1998;35:371–8. [PubMed: 9624619]

Zakany J, et al. Functional equivalence and rescue among group 11 Hox gene products in vertebral patterning. Dev Biol 1996;176:325–8. [PubMed: 8660870]

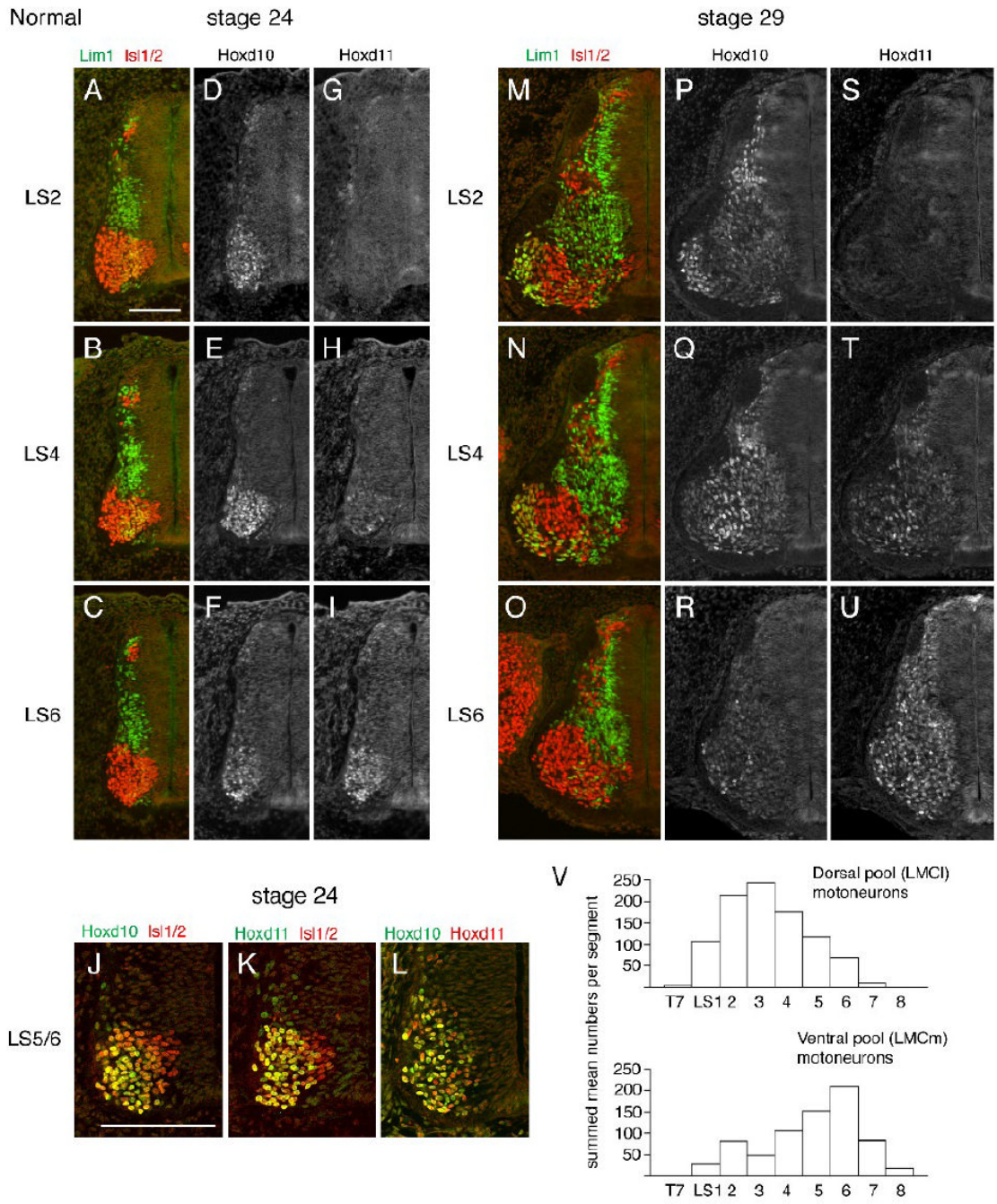

Figure 1.

Normal Hoxd10 and Hoxd11 expression domains and motoneuron subtype organization in LS spinal segments of the chick embryo. A-I. LIM and Hox expression in adjacent half cord sections at an early stage of motoneuron (MN) differentiation (stage 24). J-L. Co-expression of Hox and Isl1(2) and Hoxd10 and Hoxd11 at LS5/6 axial levels. M-U. LIM and Hox expression after motor column formation (stage 29). V. Segmental distributions of MNs projecting to dorsal and ventral limb muscles after the cell death period (stage 36, reconstructed with permission from Landmesser, 1978). Scale bars=100μm.

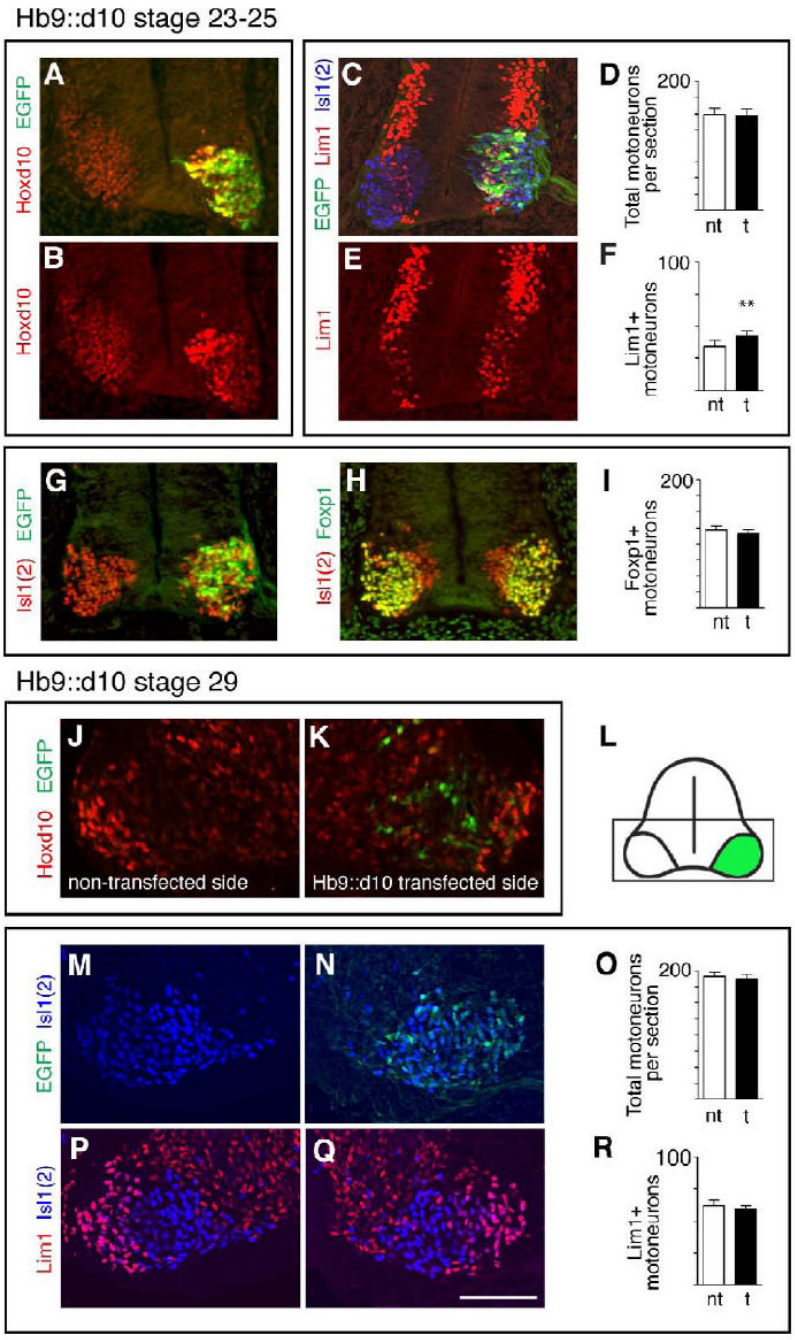

Figure 2.

Transfection with an Hb9 promoter-driven Hoxd10 construct (Hb9::d10) yields transient overexpression of Hoxd10 and a transient increase in Lim1+ MNs. A-B. Increased Hoxd10 expression and co-localization with EGFP in an LS2 section from a stage 24 Hb9::d10 embryo. C and E. EGFP and LIM expression in a triple labeled LS2 section from a stage 24 Hb9::d10 embryo. D and F. Histograms showing mean numbers of total MNs (Isl1(2)+) and Lim+ MNs per section on transfected (t) and non-transfected (nt) sides of stage 23-25 embryos. Error bars in this and all subsequent figures=s.e.m. Paired t-test comparisons of MNs on transfected and non-transfected sides: * = p< .05, ** = p< .01, *** = p< .001, numbers of embryos (3 sections

per embryo) given in Table 1. G-H. EGFP and Foxp1 expression among Isl1(2)+ MNs in adjacent LS2 sections from a stage 24 Hb9::d10 embryo. I. Histogram as in F. showing mean numbers of Foxp1+ MNs. J-L. Non-transfected and transfected sides and schematic of an LS2 section from a stage 29 Hb9::d10 embryo. Boxed area in L indicates regions shown in J-K, M-N, and P-O. Unlike stage 23-25, neither increased levels of Hoxd10, nor co-localization with EGFP are evident at stage 29. M-R. EGFP and LIM expression in a triple labeled LS2 section from a stage 29 HB9::d10 embryo and histograms as in D. and F. Scale bar=100μm.

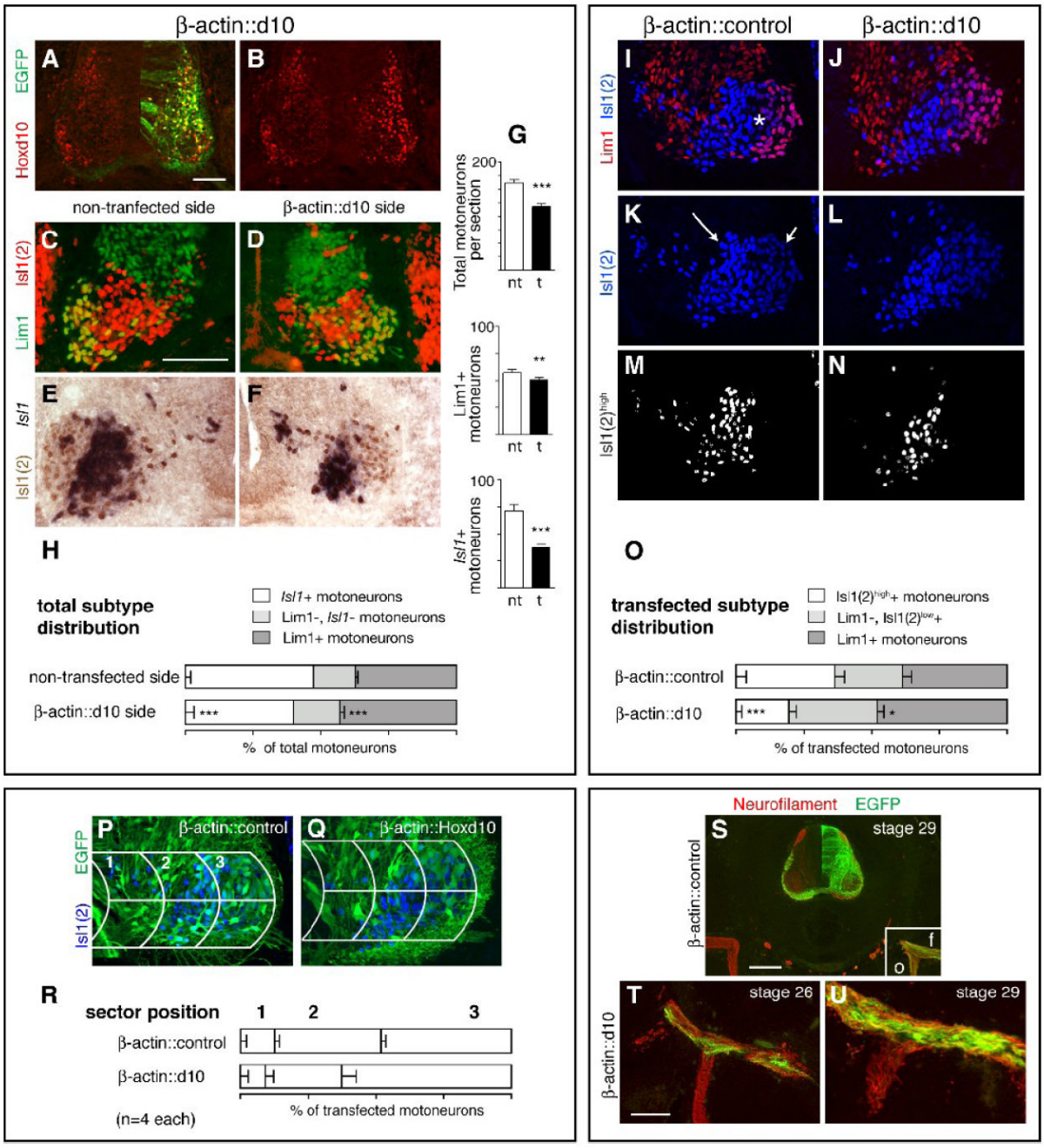

Figure 3.

Transfection with a β-actin promoter-driven Hoxd10 construct (β-actin::d10) yields sustained overexpression of Hoxd10 and a proportionate increase in Lim1+ LMCl MNs but also a substantial decrease in motor column size. A-B. Increased Hoxd10 expression and co-localization with EGFP in an LS2 section from a stage 29 β-actin::d10 embryo. C-F. LIM expression on non-transfected and transfected sides of representative LS2 sections. Sections stained with either anti-Lim1 and anti-Isl1(2) antibodies (C-D) or probed for *Isl1* mRNA in combination with anti-Isl1(2) antibody staining (E-F). G. Mean numbers of total MNs, Lim1 + MNs, and *Isl1* + MNs on non-transfected (nt) and transfected (t) sides. H. Subtype percentages

in LS2 motor columns. I-L. LIM expression in LS2 sections from β-actin::control and β-actin::d10 embryos, triple labeled with anti-Lim1, -Isl1(2), and –EGFP antibodies (EGFP shown in P and Q). Asterisk in I marks the position of Lim1- LMCl MNs. Note that these MNs as well as Lim1+ LMCl MNs stain lightly with the anti-Isl1(2) antibody (short arrow in K). In contrast more medial MNs are brightly stained (long arrow in K). M-N. Distribution of bright Isl1(2)^{high} cells after using a fluorescent intensity cut-off to subtract out Isl1(2)^{low} cells (see Materials and Methods). The position of the Isl1(2)^{high} cells approximates that of cells identified as *Isl1*+ (compare E and M). O. Subtype percentages within EGFP+ populations alone. P-R. Grid placement on sections of transfected motor columns from β-actin::control and β-actin::d10 embryos and percentages of transfected MNs in individual grid sectors. S-U. Axon trajectories in crural (anterior) limb regions from β-actin::control (S) and β-actin::d10 (T-U) embryos. Sections stained with anti-neurofilament and anti-EGFP antibodies. Boxed area in S shows the divergence of femoral (f) and obturator (o) nerve trunks and corresponds to the regions shown at higher magnification in T and U. Paired t-tests as in Fig. 2, see Table 1 for (n). Scale bars=100μm (A-Q, T-U), 200μm (S).

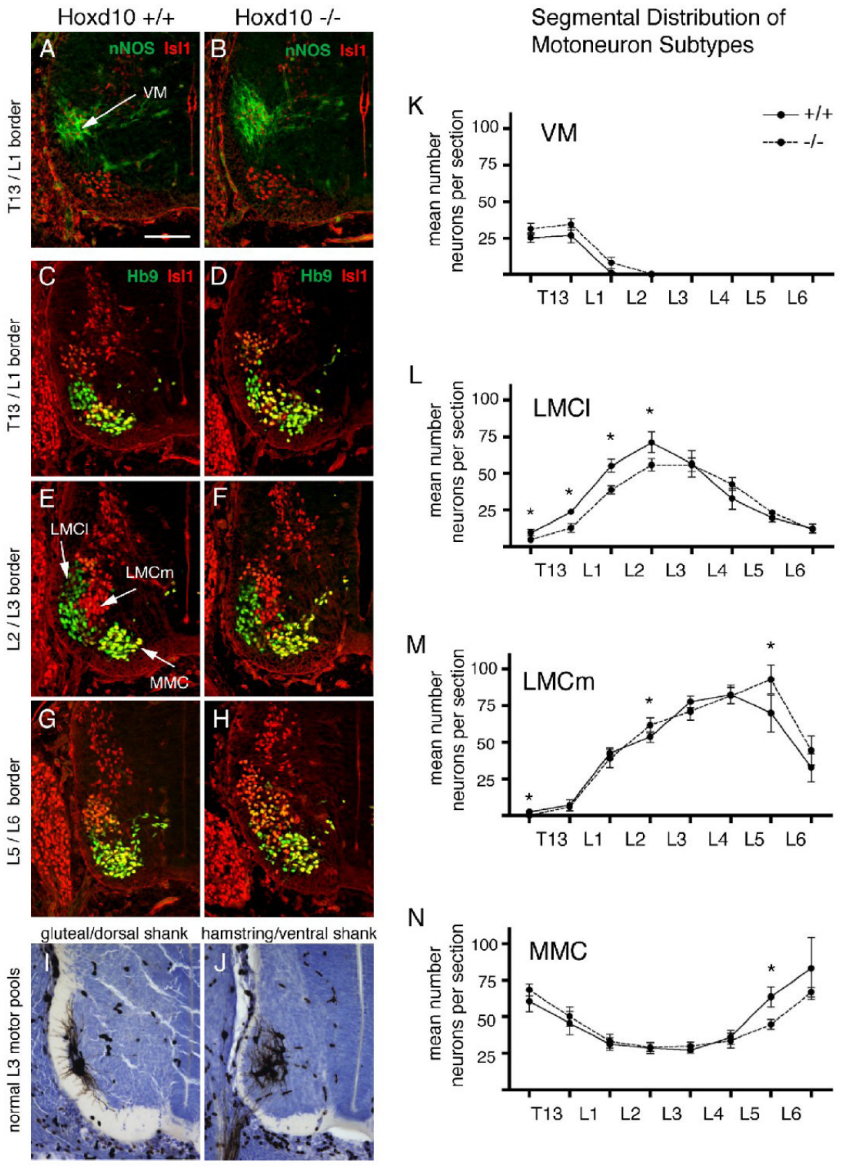

Figure 4.

Lumbar LMCl MNs are reduced in number in a loss-of-function Hoxd10 mutant mouse embryo at E12.5-E13.5. A-H. Representative sections through lumbar motor columns from Hoxd10 +/+ and Hoxd10 -/- embryos. A-B. Sections stained with anti-nNOS and anti-Isl1(2) identify visceral MNs (VM). Since anti-Isl1(2) stains only Isl1+ motoneurons in mouse embryos (Wu et al., 2008; personal observations, CLJ), this staining is referred to as Isl1 staining in the following text and images. C-H. Sections stained with anti-Hb9 and anti-Isl1 permit distinction of Hb9+, Isl1- LMCl MNs (green), Isl1+ LMCm MNs (red) and Hb9+, Isl1+ MMC MNs (yellow/green). I-J. Pool positions for gluteal/dorsal shank complex and hamstring/ventral shank complex at E13.5. K-N. Mean numbers per section of VM, LMCl, LMCm, and MMC subtypes from T13-L6. Paired t-test comparisons (n=5 wildtype and littermate pairs for VM, n=6 pairs for other motor columns), * = $p < .05$. Scale bar=100μm.

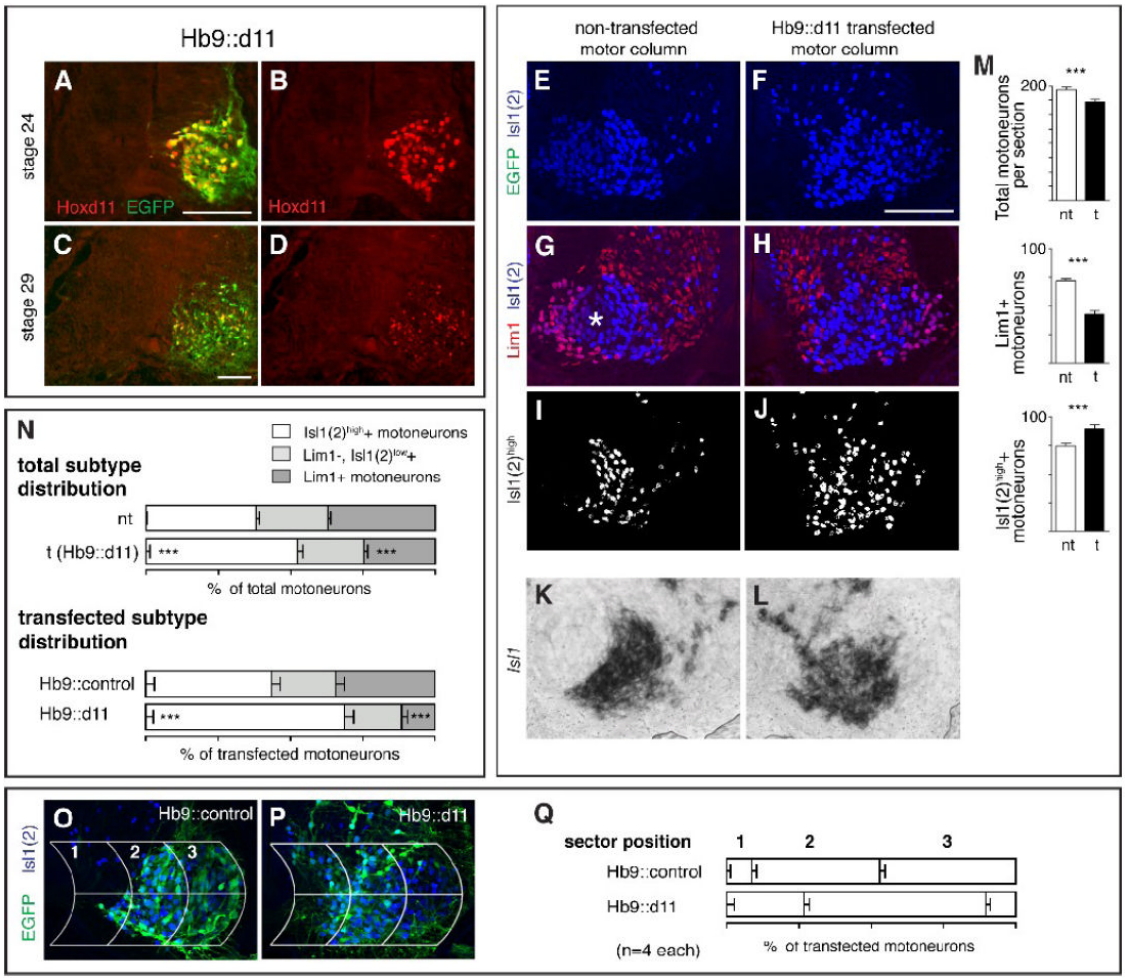

Figure 5.

Ectopic expression of Hoxd11 via transfection with an Hb9 promoter construct (Hb9::d11) leads to a shift in MN subtype complement in favor of medial subtypes. A-C. Ectopic Hoxd11 expression at rostral LS levels at stages 24 and 29 and co-localization with EGFP after transfection with Hb9::d11. E-H. LIM expression on transfected and non-transfected sides in a triple-labeled LS2 section from an Hb9::d11 embryo. (EGFP for this section shown in P). Asterisk in G denotes region of Lim1-, LMCl MNs that stain lightly with Isl1(2). I-J. Distribution of Isl1(2)^{high} cells after using a fluorescent intensity cut-off to subtract out Isl1 (2)^{low} cells. K-L. Distribution of *Isl1* mRNA on transfected and non-transfected side of LS2 from a second Hb9::d11 embryo. Note that Isl1(2)^{high} cells correspond positionally to *Isl1*+ cells. M. Histograms showing mean numbers of total MNs and subtypes per section on transfected (t) and non-transfected (nt) sides. N. Subtype percentages within transfected and non-transfected motor columns as a whole and within the transfected (EGFP+) population alone in Hb9::control and Hb9::d11 embryos. O-Q. Grid placement on sections of transfected motor columns from Hb9::control and Hb9::d11 embryos and percentages of transfected MNs in individual grid sectors. Paired t-tests as in Fig. 2. See Table 1 for (n). Scale bars=100μm.

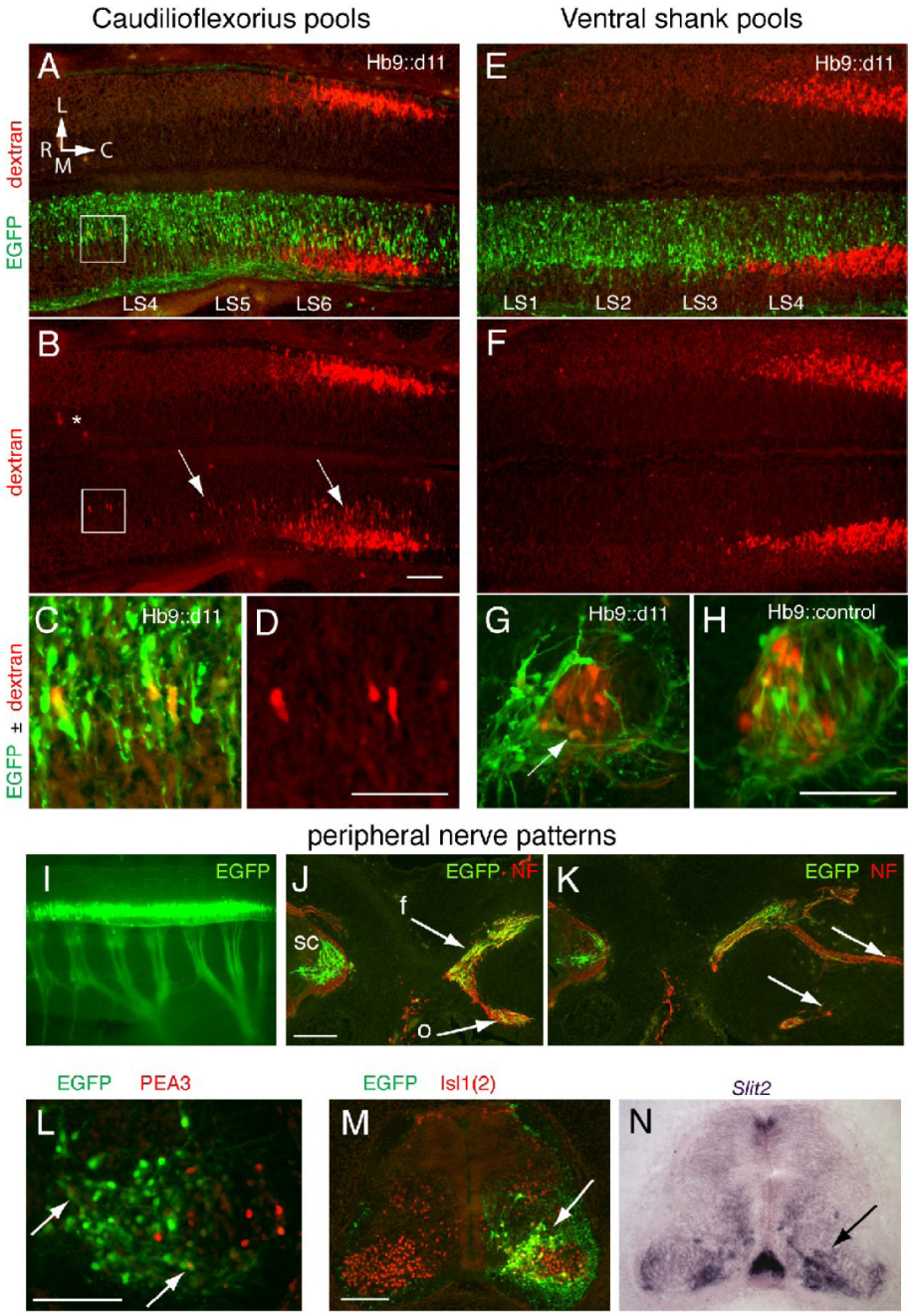

Figure 6.

MNs in rostral LS segments appear to demonstrate a caudal (caudilioflexorius) identity after transfection with Hb9::d11 but also show abnormalities in cell positioning and axon outgrowth. A. Horizontal section showing caudilioflexorius pools (dextran+ cells) on non-transfected (top) and transfected (EGFP+) sides of the ventral LS cord from a stage 30 Hb9::d11 embryo. L, lateral, M, medial, R, rostral, C, caudal. B. Dextran alone. On the non-transfected side, few if any dextran+ cells are located outside a major cluster in LS5-6. (The asterisk indicates fluorescence likely to be artifactual as it is diffuse and located well outside the motor column region.) On the transfected side, numerous dextran+ cells are positioned more medially and

rostrally than normal (box and arrows). C and D. Boxed area in A and B. On the transfected side, rostrally positioned MNs are EGFP+ and dextran+. E. and F. Ventral shank pools from an Hb9::d11 embryo. Staining and orientation as in A and B. Dextran+ cells are not present in segments rostral to the main body of the ventral shank pool. G. and H. Transverse sections through motor columns of an Hb9::d11 (G) and an Hb9::control embryo (H). In the Hb9::d11 embryo, most EGFP+ MNs occupy an extreme medial position and only a small number of EGFP+, dextran+ MNs (arrow) are evident. In the Hb9::control embryo, EGFP+ MNs are more widely distributed in the motor columns, and EGFP+, dextran+ cells, more numerous. I. EGFP expression in cord and limb nerves in whole mount of a stage 27 Hb9::d11 embryo. J-K. Transverse sections showing femoral (f) and obturator (o) nerve trunk bifurcation (J) and distal branching (K) in an Hb9::d11 embryo. Arrows indicate the presence of EGFP+ axons at proximal levels in both nerve trunks (J) but their relative absence at more distal levels (K). L. Section through a caudal LS motor column showing extensive Hoxd11 transfection but only a very small number of EGFP+, Pea3+ cells (arrows). M-N. Adjacent sections stained for EGFP, Isl1(2) and *Slit2*. *Slit2* expression is high in medial motor regions where Hoxd11-transfected cells appear to be most numerous (arrows). Scale bars=100μm, except in J-K, 200μm.

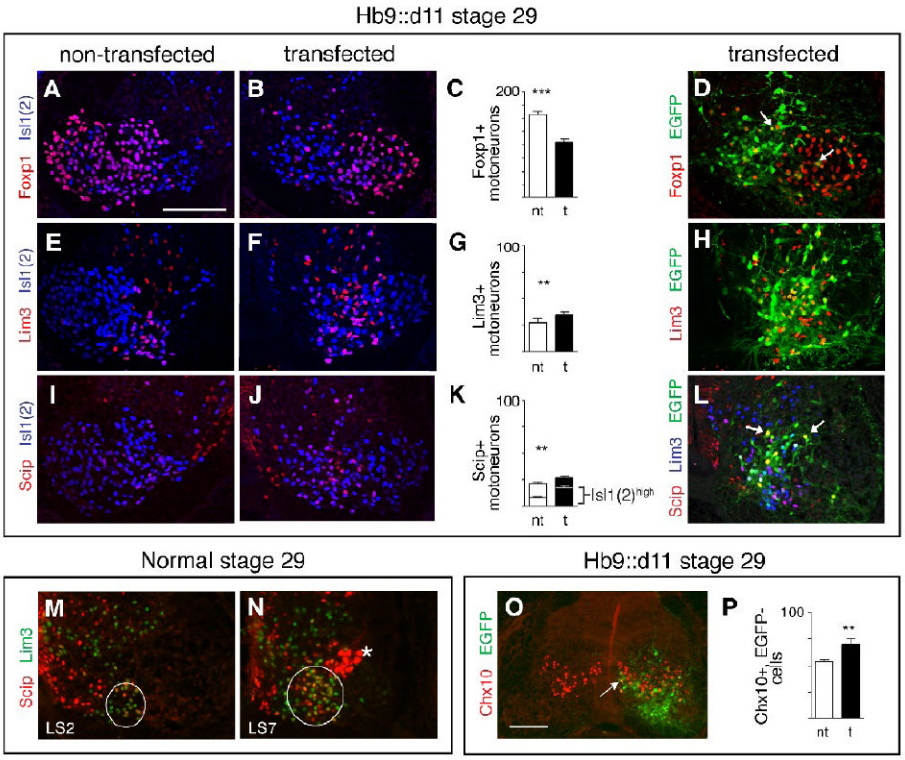

Figure 7.

Segments transfected with Hoxd11 show decreases in cells with an LMC molecular profile and increases in cells with profiles characteristic of MMC motoneurons and V2a interneurons. A-C. Distribution and numbers of Foxp1+, Isl1(2)+, LMC MNs on non-transfected and transfected sides of LS2 sections from stage 29 Hb9:d11 embryos. D. A small number of EGFP + cells on the transfected side express Foxp1+. E-G. Distribution and numbers of Lim3+, Isl1 (2)+, MMCm MNs as in A-C. H. Widely distributed EGFP+ cells on the transfected side express Lim3. I-K. Distribution and numbers of Scip+, Isl1(2) MMC MNs. Lower histogram bars (K) show Scip+, Isl1(2)^{high} cells, a molecular profile characteristic of MMCl MNs. L. EGFP+ cells on the transfected side express Scip. Not all Scip+ cells express Lim3 (arrows). M-N. In a normal stage 29 embryo, Scip+, ± Lim3+ cells are more numerous in caudal LS segments than in rostral LS segments. Circles delineate general outline of the MMC. Also unique to caudal LS sections is a cluster of Scip+, Lim3- cells (asterisk) that are LMC MNs (see Rousso et al., 2008). Note: In M-N, the cord is oriented inverse to other micrographs of non-transfected sections, for ease of comparison to experimental (see schematic). O. LS section from a stage 29 Hb9::d11 embryo showing an increase in Chx10+, EGFP-,V2a interneurons on the transfected side. In such sections small number of Chx10+ cells were occasionally EGFP + (white arrow). P. Histogram of mean numbers of Chx10+, EGFP- cells on transfected and non-transfected sides. Paired t-tests as in Fig. 2. See text for (n) and means. Scale bars=100μm, bar in A applicable to all panels except O.

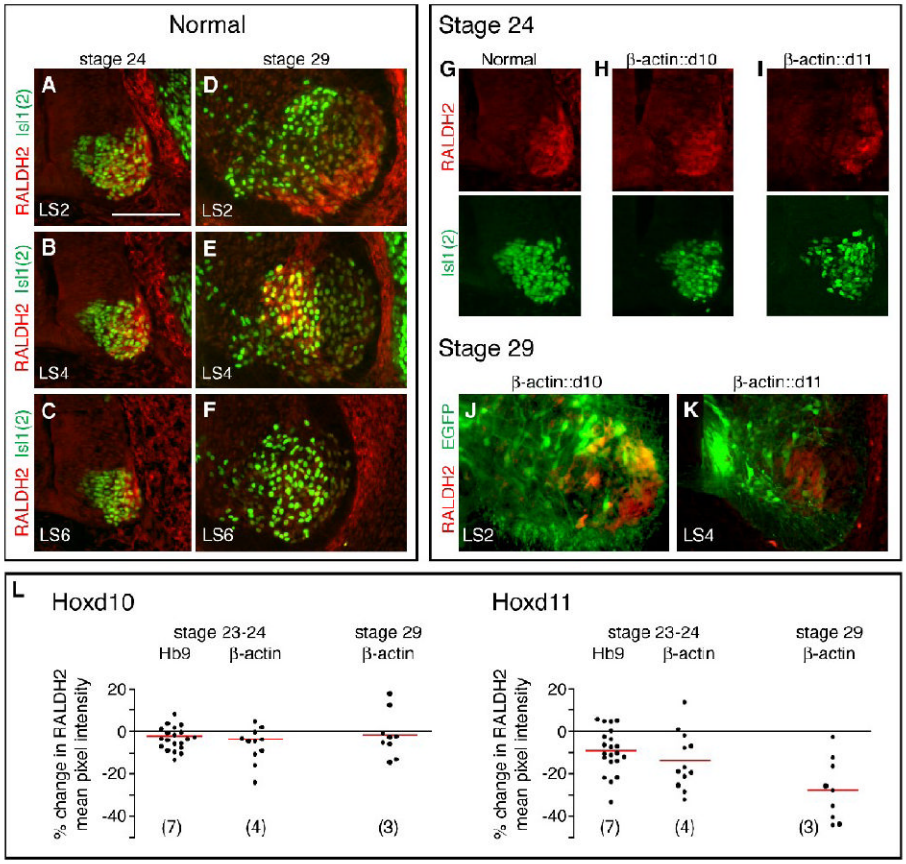

Figure 8.

RALDH2 expression is reduced in chick LS segments with ectopic expression of Hoxd11. A-F. Normal patterns of RALDH2 expression among MNs (Isl1(2)+ cells) within LS2, LS4, and LS6 sections at stage 24 (A-C) and stage 29 (D-F). G-I. RALDH2 and Isl1(2) expression at stage 24 in motor column sections from normal, β-actin::d10 and β-actin::d11 embryos. Despite a substantial population of Isl1(2)+ MNs, the Hoxd11-transfected motor column shows reduced RALDH2 expression (I). J-K. RALDH2 expression in sections from stage 29 β-actin::d10 and ß-actin::d11 embryos. RALDH2 expression is prominent in lateral EGFP+ cells in the Hoxd10-transfected section. In contrast, there is no overlap in RALDH2 and EGFP expression following Hoxd11 transfection. L. Plots of % change in fluorescence intensity on transfected and non-transfected sides of anti-RALDH2 stained sections. Average fluorescence intensity was determined for circumscribed motor areas to correct for any differences in motor column size on transfected and non-transfected sides. Each dot=1 section, 0=no difference between transfected and non-transfected sides, negative number=decrease on transfected side. Red bars=mean % change in fluorescence for embryos transfected with the same Hox construct and sacrificed at the same stage. (Numbers and paired t-test p values in text) Scale bar=100 μm.

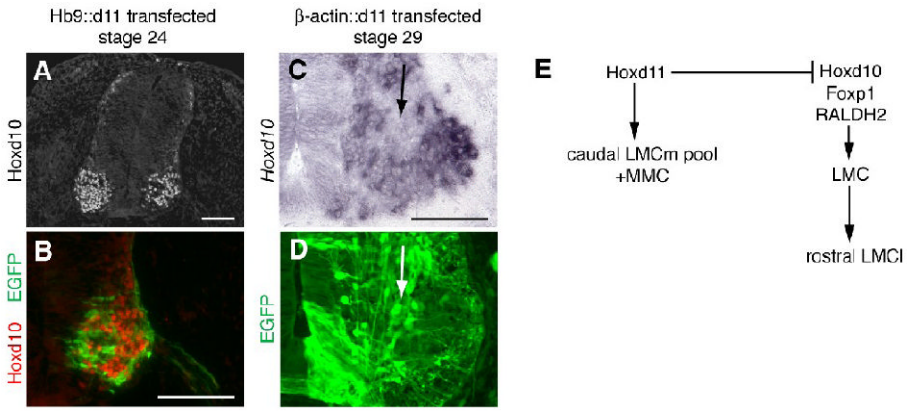

Figure 9.

Repression of Hoxd10 by Hoxd11 and summary schematic of Hox influences on MN subtype complement along the rostrocaudal axis of the LS cord. A-B. Transverse section from a stage 24 Hb9::d11 embryo showing absence of Hoxd10 protein in Hoxd11-transfected (EGFP+) cells. C-D. Transverse views of the rostral LS cord from a stage 29 β-actin::d11 embryo. Adjacent sections show a reduction in *Hoxd10* expression in motor regions rich in EGFP+ cells (arrows). E. Proposed influences of Hoxd11 and Hoxd10 on LS MN differentiation. Scale bars=100 μm.

Table 1

Quantification of motoneuron transcription factor expression in control and Hox-electroporated chick LS segments

Experimental subsets	# of motoneurons				% of motoneurons			% of transfected motoneurons			
	n[1]	nt[2]	t		nt	t		n	control[4]	Hox	
Hb9::Hoxd10 - Stage 23-25											
LS2											
Isl1(2)+	4	149±9	149±9								
Lim1+	4	34±5	43±1	**[3]	22±2	29±2	**			42±3	
Foxp1+	6	123±6	117±6								
Hb9::Hoxd10 - Stage 29											
LS2											
Isl1(2)+	4	191±7	187±10								
Lim1+	4	62±4	59±3		32±1	32±2					
Isl1(2)^{high}+	4	72±3	72±5		38±1	39±2					
b-actin::Hoxd10 - Stage 29											
LS2											
Isl1(2)+	5	162±5	119±5	***							
Lim1+	5	58±3	51±3	**	35±1	43±2	***	4	39±3	48±2	*
Isl1+	4	72±6	37±4	***	51±3	40±3	***	4	36±4	19±2	***
LS5											
Isl1(2)+	4	181±5	119±7	***							
Lim1+	4	43±3	40±2		24±1	34±2	***				
Hb9::Hoxd11 - Stage 29											
LS2											
Isl1(2)+	6	194±5	172±5	***							
Lim1+	6	72±2	43±3	***	37±1	25±1	***	4	34±3	12±2	***
Isl1(2)^{high}+	6	74±2	90±3	***	38±1	52±1	***	4	44±3	69±3	***
Foxp1+	5	158±5	106±6	***							
Lim3+	6	27±4	35±2	**							
Scip+	4	21±1	27±2	**							
Scip+/Foxp1+	5	16±1	15±1								
Scip+/Isl1(2)high+	4	9±1	17±2	***							

Experimental subsets	# of motoneurons				% of motoneurons			% of transfected motoneurons			
	n[1]	nt[2]	t		nt	t		n	control[4]	Hox	
b-actin::Hoxd11 - Stage 29											
LS2											
Isl1(2)+	5	146±7	111±5	***							
Lim1+	5	57±4	40±2	***	39±1	36±1	***	4	39±3	16±3	***
Isl1+	4	61±3	62±5		44±2	54±3	*	4	36±4	67±5	***
LS5											
Isl1(2)+	3	167±10	141±12	**							
Lim1+	3	45±4	25±2	**	27±3	19±2	**				
Hb9::control - Stage 29											
LS2											
Isl1(2)+	6	204±8	186±8								
Lim1+	6	79±5	71±3		38±1	38±1					
Isl1(2)^{high}+	6	76±4	73±4		37±1	39±1					
b-actin::control - Stage 29											
LS2											
Isl1(2)+	5	158±6	160±3								
Lim1+	5	63±3	61±3		40±1	38±2					

[1] n=number of embryos analyzed. In each embryo, three non-adjacent sections within the same segment were counted.

[2] nt, non-transfected side of the spinal cord; t, transfected side of the spinal cord.

[3] Asterisks represent signficance, based on paired or un-paired t-tests.

* p<0.05;

** p<0.01;

*** p<0.001.

[4] The term “control” describes embryos electroporated with a control construct expressing EGFP alone. “Hox” describes embryos electroporated with a construct encoding EGFP and either Hoxd10 or Hoxd11.